

อิทธิพลของตำแหน่งที่ให้อากาศต่อการกระจายตัวของฟองอากาศและการถ่ายเทมวลระหว่าง
ก๊าซและของเหลวในถังสัมผัสแบบอากาศยกชนิดไหลวนภายใน



นางสาวสนธิ์ บุญสุวรรค์

วิทยานิพนธ์นี้เป็นส่วนหนึ่งของการศึกษาตามหลักสูตรปริญญาวิศวกรรมศาสตรมหาบัณฑิต

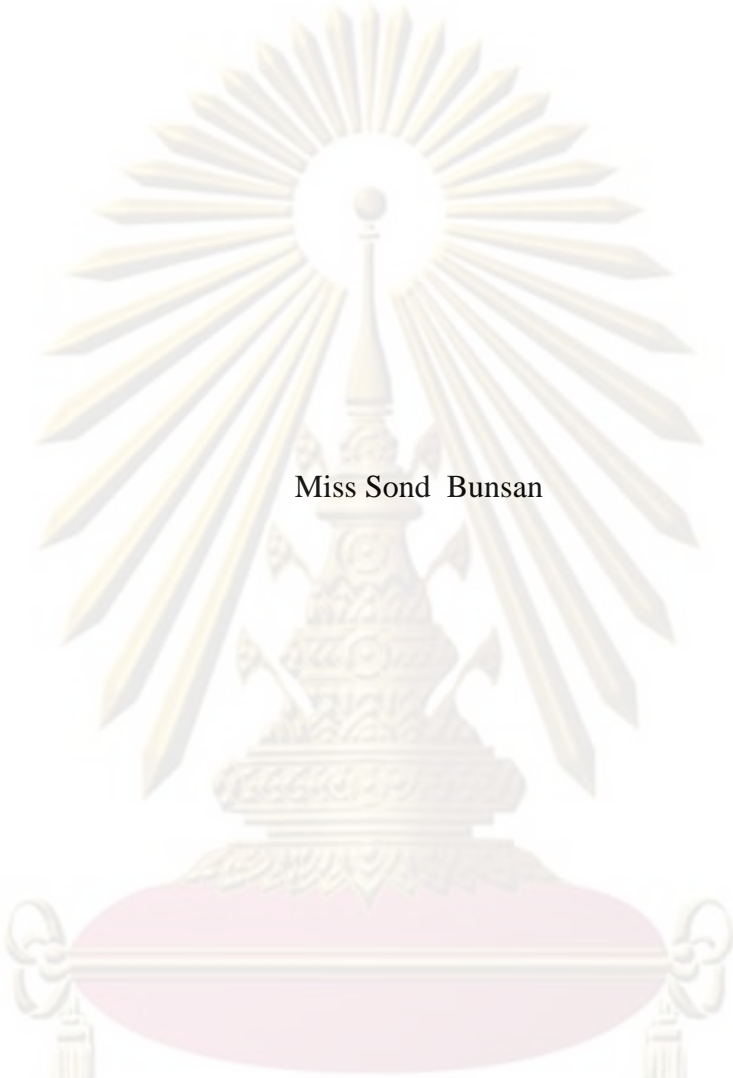
สาขาวิชาวิศวกรรมเคมี ภาควิชาวิศวกรรมเคมี

คณะวิศวกรรมศาสตร์ จุฬาลงกรณ์มหาวิทยาลัย

ปีการศึกษา 2552

ลิขสิทธิ์ของจุฬาลงกรณ์มหาวิทยาลัย

EFFECT OF SPARGER POSITION ON BUBBLE SIZE DISTRIBUTION AND
GAS-LIQUID MASS TRANSFER IN INTERNAL AIRLIFT CONTACTORS



Miss Sond Bunsan

A Thesis Submitted in Partial Fulfillment of the Requirements
for the Degree of Master of Engineering Program in Chemical Engineering

Department of Chemical Engineering

Faculty of Engineering

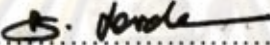
Chulalongkorn University

Academic Year 2008

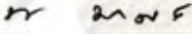
Copyright of Chulalongkorn University

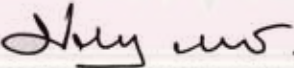
Thesis Title EFFECT OF SPARGER POSITION ON BUBBLE SIZE
DISTRIBUTION AND GAS-LIQUID MASS TRANSFER IN
INTERNAL AIRLIFT CONTACTORS
By Miss Sond Bunsan
Field of study Chemical Engineering
Thesis Advisor Associate Professor Prasert Pavasant, Ph.D.

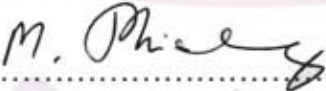
Accepted by the Faculty of Engineering, Chulalongkorn University in
Partial Fulfillment of the Requirements for the Master's Degree



.....Dean of the Faculty of Engineering
(Associate Professor Boonsom Lerdkhironwong, Dr.Ing.)

THESIS COMMITTEE


.....Chairman
(Associate Professor Tharathon Mongkhonsi, Ph.D.)


.....Thesis Advisor
(Associate Professor Prasert Pavasant, Ph.D.)


..... Examiner
(Associate Professor Muenduen Phisalaphong, Ph.D.)


..... External Examiner
(Associate Professor Navadol Laosiripojana, Ph.D.)

ศูนย์พัฒนาศึกษา
จุฬาลงกรณ์มหาวิทยาลัย

5070475321 : MAJOR CHEMICAL ENGINEERING

KEYWORDS : PNEUMATIC REACTOR / REACTOR DESIGN / BUBBLE COLUMN / HYDRODYNAMIC BEHAVIOR / HYDRODYNAMICS

SOND BUNSAN : EFFECT OF SPARGER POSITION ON BUBBLE SIZE DISTRIBUTION AND GAS-LIQUID MASS TRANSFER IN INTERNAL AIRLIFT CONTACTORS. THESIS ADVISOR: ASSOC PROF. PRASERT PAVASANT, Ph.D., 71 pp.

This work was set out to investigate the influence of sparger position on the bubble size distribution in internal loop airlift contactors. To complete the examination, the effects of other main design/operating parameters, i.e. the ratio between cross-sectional areas of downcomer and riser (A_d/A_r) and the superficial gas velocity, were also considered. The aeration in the ALC was achieved via the PVC ring sparger. The number of holes in the sparger was fixed at 60. The air flow rate was controlled in a range of superficial gas velocity, u_{sg} , from 4 to 10 cm s^{-1} . The ratios between cross-sectional areas were varying from 1.4 to 0.9. The sparger position was varied by changing the position of annulus sparger (0, 6 and 12 cm above the bottom of the contactor). A photographic technique was used to measure the bubble size and its distribution. The results revealed that the Sauter mean diameter of bubble was the smallest when the sparger was located at base of the reactor, and became larger when the sparger was moved to higher positions. It should be noted that at the lowest position, the sparger position was lower than the draft tube, therefore the recirculating fluid from the downcomer pushed the newborn bubbles towards the wall of the reactor and bubble breakage was observed. In addition, bubble size was also controlled by other flow conditions in the system, especially the superficial gas velocity (u_{sg}), where an increase in u_{sg} decreased the bubble size due to the induction of high turbulence which rendered the bubble breakup. The system operated with smaller riser area had a higher level of turbulence, thus, the average bubble size was found to be smaller than system with larger riser area. At the bottom section of the reactor, the Sauter mean bubble diameter appeared to be larger than those at the middle and top sections. In terms of gas-liquid mass transfer, the sparger at its lowest position provided the highest level of overall volumetric mass transfer coefficient in the system. The specific interfacial area at the lowest sparger position was also found to be higher than other positions which suggested that this specific interfacial area could have strong positive impact on the gas-liquid mass transfer.

Department : Chemical Engineering

Student's Signature สนธิ บุนสันท

Field of Study : Chemical Engineering

Advisor's Signature Prasert Pavasant

Academic Year : 2009

ACKNOWLEDGEMENTS

This thesis will never have been completed without the help and supports of many people who are gratefully acknowledged here. Firstly, I would like to express my sincere gratitude to Associate Professor Prasert Pavasant, my advisor, for his suggestions, guidance, warm encouragement and generous supervision throughout my master program. I am also grateful to Associate Professor Dr. Tharathon Mongkhonsi, chairman of the committee, Assistant Professor Dr. Sarawut Rimduisit, Assistant Professor Dr. Muenduen Phisalaphong and Associate Professor Dr. Navadol Laosiripojana for their helpful and many valuable comments.

I would like to gratefully thank the Department of Chemical Engineering that gave a chance for studying in the field of engineering. I cannot forget to express my thankfulness to my lovely friends in Biochemical Engineering Research Laboratory, Chulalongkorn University for fulfilling the happiness inside.

Most of all, I would like to express my sincere indebtedness to my family for their worth supports throughout my Master courses.



ศูนย์วิทยทรัพยากร
จุฬาลงกรณ์มหาวิทยาลัย

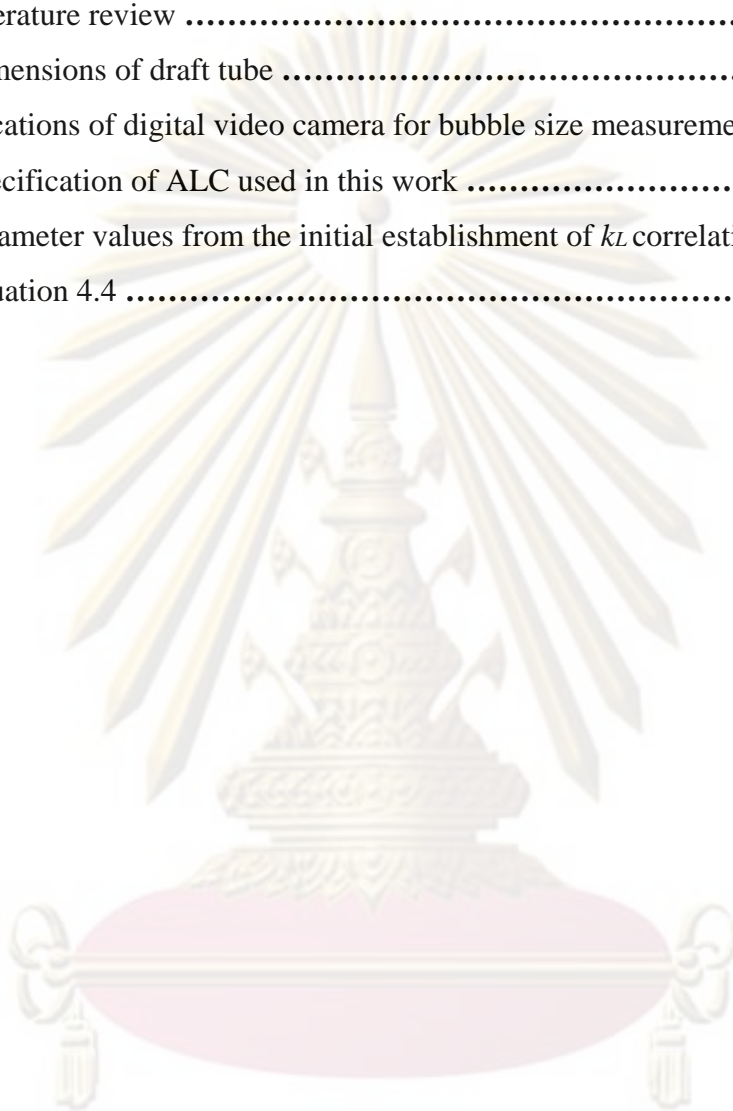
CONTENTS

	Page
ABSTRACT IN THAI	iv
ABSTRACT IN ENGLISH	v
ACKNOWLEDGEMENTS	vi
TABLE OF CONTENTS	vii
CONTENTS	vii
LIST OF TABLES	ix
LIST OF FIGURES	x
CHAPTER 1 INTRODUCTION	
1.1 Motivations.....	1
1.2 Objectives.....	2
1.3 Scopes of this work.....	3
CHAPTER 2 BACKGROUNDS AND LITERATURE REVIEWS	
2.1 Backgrounds : Airlift contactors.....	6
2.2 Three main regions of airlift contactors.....	6
2.3 Hydrodynamics in airlift contactors.....	7
2.3.1 Liquid velocity.....	7
2.3.2 Gas holdup.....	8
2.4 Gas-liquid mass transfer.....	9
2.5 Bubble size distribution.....	10
CHAPTER 3 MATERIALS AND METHODS	
3.1 Experimental setup.....	16
3.2 Experiments procedures.....	17
3.2.1 Measurement of bubble size distribution.....	17
3.2.2 Liquid velocity measurement.....	17
3.2.3 Mass transfer coefficient measurement.....	18
3.2.4 Gas holdup measurement.....	19

	Page
3.3 Calculations	
3.3.1 Bubble size calculation	20
3.3.2 Liquid velocity	20
3.3.3 Volumetric mass transfer coefficient calculation	20
3.3.4 Gas holdup calculation	21
CHAPTER 4 RESULTS AND DISCUSSION	
4.1 Error compensation in photographic technique	27
4.2 Bubble size distribution as a function of sparger position	27
4.3 Bubble size distribution as a function of superficial gas velocity	28
4.4 Average bubble size as a function of the ratio between downcomer and riser cross-sectional area	29
4.5 Axial average bubble size in airlift contactor	29
4.6 Overall volumetric mass transfer coefficient (k_{La}) in airlift contactor	30
4.7 Empirical models for the prediction of the Sauter mean bubble diameter of various parameters	34
CHAPTER 5 CONCLUSIONS, CONTRIBUTIONS AND RECOMMENDATIONS	
5.1 Conclusions	52
5.2 Contributions	53
5.3 Recommendations	53
REFERENCES	54
APPENDICES	58
BIOGRAPHY	71

LIST OF TABLES

Tables	Page
Table 2.1 Relative performance of external and internal airlift bioreactors.....	12
Table 2.2 Literature review	13
Table 3.1 Dimensions of draft tube	24
Table 3.2 Locations of digital video camera for bubble size measurement	24
Table 3.3 Specification of ALC used in this work	24
Table 4.1 Parameter values from the initial establishment of k_L correlation in Equation 4.4	35



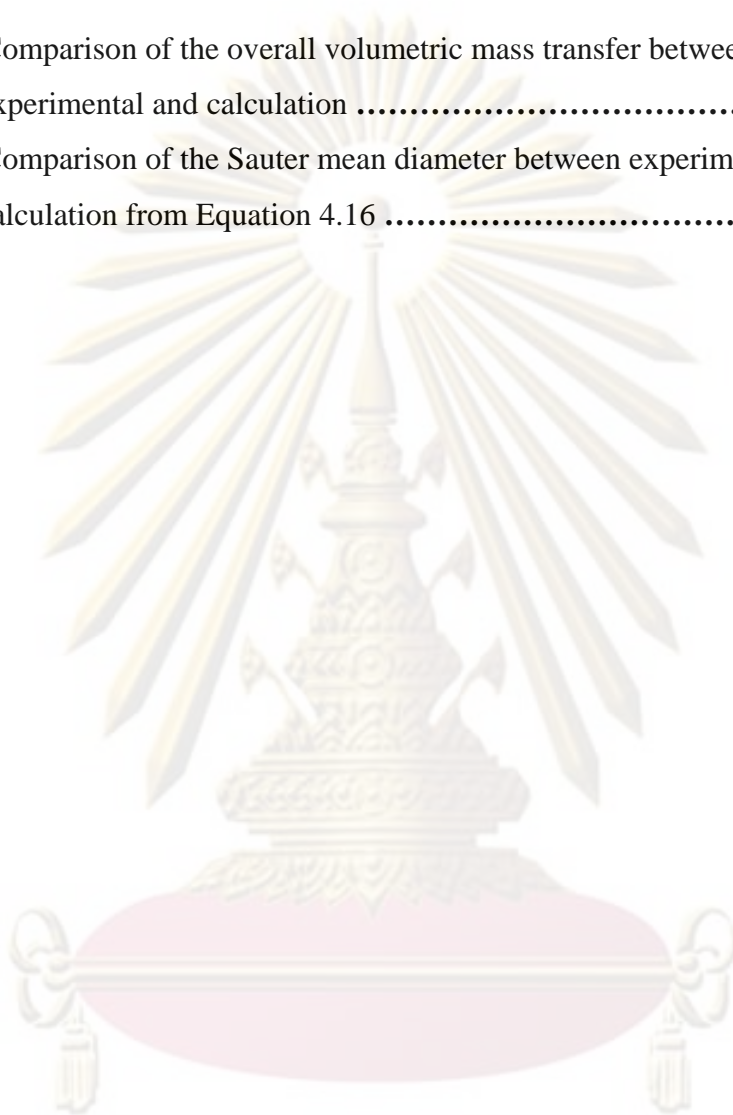
ศูนย์วิทยทรัพยากร
จุฬาลงกรณ์มหาวิทยาลัย

LIST OF FIGURES

Figure	Page
Figure 1.1 Internal-loop airlift contactors	4
Figure 1.2 External-loop airlift contactors	5
Figure 2.1 Schematic flow directions in airlift system	15
Figure 3.1 Schematic diagrams of concentric internal loop airlift contactor employed in this work	25
Figure 3.2 Major and minor axes of bubble images	26
Figure 4.1 An example of photographs of bubbles obtained from this measurement technique	36
Figure 4.2 The effect of sparger position on gas distribution in airlifts	37
Figure 4.3 Bubble size distribution at various superficial gas velocity in ALC-1	38
Figure 4.4 Bubble size distribution at various superficial gas velocity in ALC-2	39
Figure 4.5 Bubble size distribution at various superficial gas velocity in ALC-3	40
Figure 4.6 Bubble size distribution at various superficial gas velocity in ALC-4	41
Figure 4.7 Bubble size distribution at various superficial gas velocity in ALC-5	42
Figure 4.8 Relationship between the average bubble diameter and superficial gas velocity along axial location in all ALC	43
Figure 4.9 Relationship between the average bubble diameter and superficial gas velocity in all ACL	44
Figure 4.10 Relation between different axial location and superficial gas velocity	45
Figure 4.11 Relationship between the overall volumetric mass transfer coefficients and superficial gas velocity	46
Figure 4.12 Relationship between the riser liquid velocity and superficial gas velocity	47
Figure 4.13 Relationship between the overall gas holdup and superficial gas velocity	48

จุฬาลงกรณ์มหาวิทยาลัย

Figure	Page
Figure 4.14 Relationship between the specific interfacial area in riser and superficial gas velocity	49
Figure 4.15 Comparison of the overall volumetric mass transfer between experimental and calculation	50
Figure 4.16 Comparison of the Sauter mean diameter between experimental and calculation from Equation 4.16	51



ศูนย์วิทยทรัพยากร
 จุฬาลงกรณ์มหาวิทยาลัย

CHAPTER 1

Introduction

1.1 Motivations

Airlift reactors are widely employed in many biochemical processes such as aerobic fermentation and wastewater treatment. The advantages of airlift reactors include efficient mixing, avoiding destruction in shear sensitive organisms, requiring low energy input, and simple construction. The intrinsic complicated hydrodynamic structures induced by bubble motion have been recognized to be the key factors responsible for the mass transfers (Lin et al., 2005). In fact, an airlift reactor is a modified bubble column reactor. The riser section of an airlift reactor can be regarded as a bubble column. On account of the additional loop for liquid circulation, fluid dynamic conditions are altered causing the operation range of the airlift reactor to be different from that of the bubble column (Merchuk et al., 1986). The main advantages of the airlifts over bubble columns are improved mixing and actually higher mass transfer coefficient in some instances particularly in the system with three phases. This latter is possible because of the very high gas velocity which may be used in the airlifts (Chisti, 1989).

Two basic classes of the airlifts may be distinguished: (i) the internal-loop airlifts where what would otherwise be a simple bubble column has been split into a riser and downcomer by an internal baffle as shown in Fig 1.1; and (ii) the external- or outer-loop airlift reactors where the riser and downcomer are two separate tubes connected by horizontal conduits near the top and the bottom of the main column as shown in Fig 1.2.

Some of the important hydrodynamic parameters of the airlift reactors are gas holdup, gas-liquid mass transfer and bubble size distribution. The influences of operating variables on these parameters are essential for proper design and scale-up of such reactors. The distance between the end of the draft tube and the base plate of the reactor body determined the rate of liquid and gas circulation in the loop. The mass transfer phenomena and other hydrodynamic

parameters require the information of the bubble size distribution (Majumder et al., 2006) as it is the main parameter used to determine the level of interfacial mass transfer area which then provides the basics for the estimate of other hydrodynamic parameters such as slip velocity.

Up to now, the study of the local hydrodynamics parameters, such as overall mass transfer rate, liquid velocity etc., in internal-loop airlift reactor has been rare. In addition, the sparger position in the reactor has received only minimal attention.

The principal objective of this study is to investigate how parameters, such as, bubble size distribution, liquid velocity and gas-liquid mass transfer are affected by various air flow rate, sparger position, area ratio between gas sparger and the riser and various the ratio between downcomer and riser cross-sectional areas (A_d/A_r).

1.2 Objectives

- 1.2.1 To investigate the effect of sparger position on bubble size distribution in the internal airlift contactors.
- 1.2.2 To investigate the effect of sparger position on gas-liquid mass transfer in the internal airlift contactors.
- 1.2.3 To investigate the effect of the ratio between cross-sectional areas of downcomer and riser (A_d/A_r) on bubble size distribution and gas-liquid mass transfer in the internal airlift contactors.
- 1.2.4 To investigate empirical correlations to predict hydrodynamic behavior and mass transfer rate in internal airlift contactors.

ศูนย์วิจัยทรัพยากร

จุฬาลงกรณ์มหาวิทยาลัย

1.3 Scopes of this work

- 1.3.1 The experiments are operated in gas-liquid system where tap water is used as a liquid phase and ambient air as a gas phase.
- 1.3.2 In all investigations, the airlift contactor systems are subjected to the following assumptions:
 - 1.3.2.1 The system is isothermal and operated at room temperature, where the effect of the dynamics of the dissolved oxygen at electrode is negligible.
 - 1.3.2.2 The system is operated at atmospheric pressure.
- 1.3.3 The air flow-rate is controlled in a range of superficial gas velocity from 4.0 to 10.0 cm/s.
- 1.3.4 The height of the sparger position is varied in a range of 0-12cm.
- 1.3.5 Air is sparged into the annular section using ring sparger with 60 hole areas.
- 1.3.6 The investigations of mass transfer characteristics are restricted to oxygen transfer only.



ศูนย์วิจัยทรัพยากร
จุฬาลงกรณ์มหาวิทยาลัย

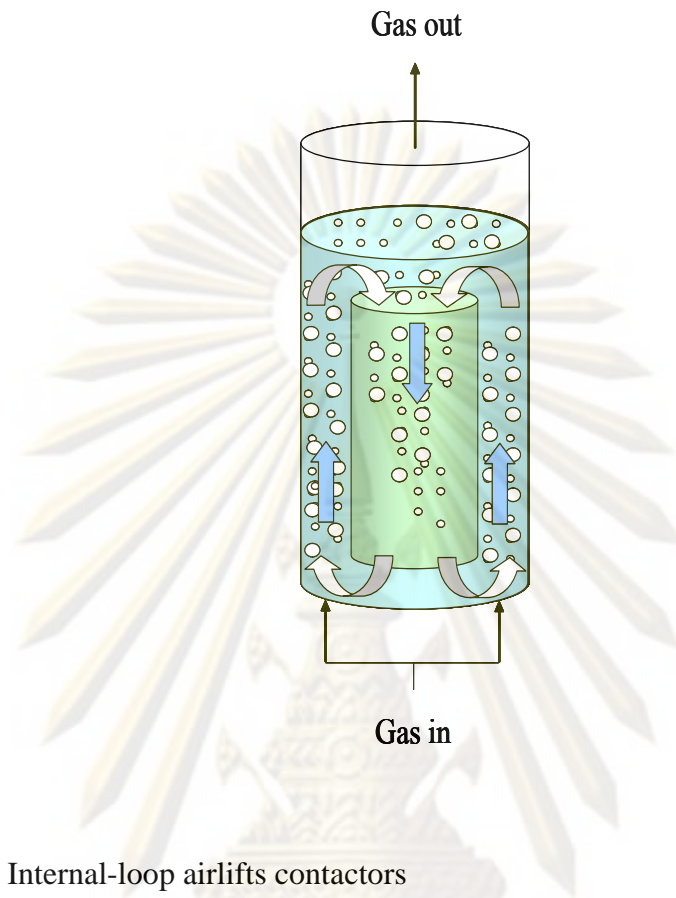


Figure 1.1 Internal-loop airlifts contactors

ศูนย์วิทยทรัพยากร
จุฬาลงกรณ์มหาวิทยาลัย

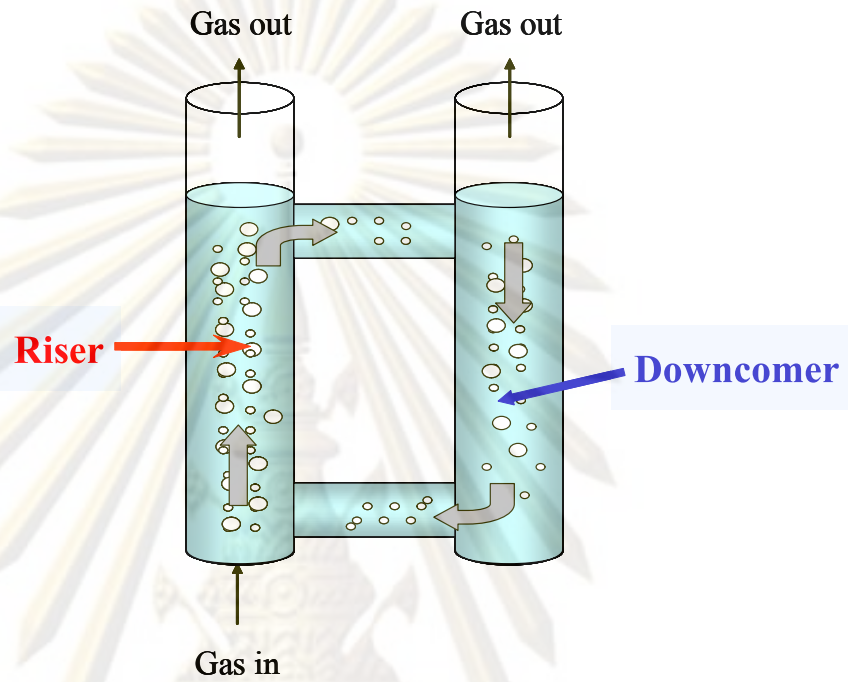


Figure 1.2 External-loop airlifts contactors

ศูนย์วิทยทรัพยากร
จุฬาลงกรณ์มหาวิทยาลัย

CHAPTER 2

Backgrounds and Literature Reviews

2.1 Backgrounds: Airlift contactor

An airlift reactor is a modified bubble column reactor. Based on the configuration of the geometry, airlift reactors are generally classified into two main categories: internal loop and external loop. The comparison of the performance of the internal and the external configurations of airlift reactor can be made in terms of various indicators, as summarized in [Table 2.1](#).

On account of the additional loop for liquid circulation, fluid dynamic conditions are altered causing the operation range of the airlift reactors to be different from bubble column. The main difference between the airlift and the bubble column is that the rate of liquid circulation in airlift depends on the gas flow rate, where the liquid flow in bubble column is independent from gas flow. The airlift reactors have been widely designed for cultivation of biological organism as they have low shear stress and good solids suspending power.

The advantages of the airlift reactors are better liquid circulation, large gas liquid interfacial areas, higher mass transfer rate, low power consumption, short mixing time, mild mixing condition and well mixing efficiency.

2.2 Three main regions of airlift contactors

(Schematic flow directions shown in [Figure 2.1](#))

Airlift contactors consist of three main sections:

- 1) Riser: Gas is introduced into this section. Due to energy/momentum transfer, liquid flows co-currently with gas bubbles upwards along the length of the contactor.
- 2) Gas-liquid separator: Most gas bubbles disengage from the liquid pool at this section. The degassed fluid becomes heavier than that in the riser and starts to move down into the downcomer.
- 3) Downcomer: This section allows the downflow of liquid. Some small bubbles can also be dragged down the downcomer by the inertial force of

the circulating liquid. The fluid recirculates back to the riser again at the bottom of the contactor.

2.3 Hydrodynamics in airlift contactors

2.3.1 Liquid velocity

The liquid circulation occurs due to two main causes. Firstly, the upward movement is induced from the energy/momentum balance from the input gas at the bottom of the contactor. Secondly, the differences in the fluid densities in riser and downcomer can also cause substantial liquid movement between the two sections. Generally, liquid velocity is measured in terms of linear liquid velocity defined as:

$$u_L = \frac{x_L}{t} \quad (2.1)$$

where x is the path length and t is the average time for one complete movement. The superficial liquid velocity is the velocity calculated based on the area of the empty column (with no barrier) and therefore is different from the true linear velocity. The true velocity is always higher than superficial velocity as the area for the liquid movement is always blocked by the gas bubbles. The linear liquid velocities in riser, v_{Lr} , and in downcomer, v_{Ld} can be related to superficial velocity according to the following expressions:

$$v_{Lr} = \frac{u_{Lr}}{1 - \varepsilon_r} \quad (2.2)$$

and

$$v_{Ld} = \frac{u_{Ld}}{1 - \varepsilon_d} \quad (2.3)$$

There are various techniques to measure linear liquid velocity (v_{Lr} , v_{Ld}) such as a classic, color tracer injection method.

The superficial velocities are measured either in the riser (u_{Lr}) or in the downcomer (u_{Ld}) where the relationship between the two quantities can be expressed using the mass balance principle as:

$$u_{Lr} A_r = u_{Ld} A_d \quad (2.4)$$

This allows the estimation of one liquid velocity when the other is known. The liquid velocity in internal loop airlift was often reported to be higher than that in external loop.

2.3.2 Gas holdup

The volume fraction of the gas-phase in the gas-liquid dispersion is known as the gas void fraction or the gas holdup. The overall gas holdup (ε) is the ratio between the volume of gas phase and the total volume of reactor which can be expressed as:

$$\varepsilon = \frac{V_G}{V_G + V_L} \quad (2.5)$$

where: V_G is the gas volume and V_L the liquid volume.

In airlift contactors, individual riser and downcomer gas holdups (ε_r and ε_d), can also be identified and are related to the overall gas holdup through the following equation:

$$\varepsilon_o = \frac{A_r \varepsilon_r + A_d \varepsilon_d}{A_r + A_d} \quad (2.6)$$

Eq.(2.6) is derived for contactors with uniform cross-sections of the riser and the downcomer. This equation is exact for internal loop airlifts and it is applicable also to external loop when the dispersion heights in the riser and the downcomer are nearly the same.

Moreover, the calculation for gas holdup can be estimated by using information on superficial gas velocity and cross-section area ratio. [Wongsuchoto \(2003\)](#) summarized the empirical correlations proposed by various researchers on the estimation on gas holdup in airlift contactors. [Table 2.2](#) further summarizes some recent work regarding the estimate of gas holdup in the airlift reactors.

2.4 Gas-liquid mass transfer

One of the most important factors for the operation of bioreactors is the gas-liquid mass transfer. As general criteria in most aerobic cultures, cells need oxygen to stay alive and active. However, the level of dissolved oxygen in the culture is always limited by thermodynamics where solubility of oxygen in water is only around 7 ppm at ambient condition. The rate at which oxygen is dissolved into the water is therefore an important key step in accelerating cell growth, and it is essential to know the behavior of the system in transferring gas between the two phases.

The overall volumetric mass transfer coefficient (or $k_L a$) is a combination of two variables, i.e. k_L and a . k_L is the mass transfer coefficient and a is the specific surface area for mass transfer. The determination of each of these parameters requires a tedious experimental work on the measurement of bubble size distribution and this is often not practical in large scale systems. A more conventional method of determining the rate of gas-liquid mass transfer is to find the product of the two quantities, $k_L a$. To determine this parameter, the method based on a dynamic approach of oxygen is employed. Oxygen balance performed across an aerated bioreactor in which a living culture is actively growing is formulated:

$$\frac{dC_L}{dt} = k_L a (C_L^* - C_L) - r_{O_2} \quad (2.7)$$

where C_L is the dissolved oxygen concentration, C_L^* the dissolved oxygen concentration in equilibrium with partial pressure of oxygen in the air, $k_L a$ the volumetric oxygen transfer coefficient, and r_{O_2} the rate of oxygen used per unit mass of organisms. For systems without reaction, r_{O_2} disappears and Equation (2.7) becomes

$$\frac{dC_L}{dt} = k_L a (C_L^* - C_L) \quad (2.8)$$

The overall volumetric oxygen transfer coefficient $k_L a$ was determined by the dynamic gassing-in method as used previously by the **K.H. Choi (1996)** they investigated for the two airlift reactors was comparable; the

bubble column was higher values of k_{La} than airlift reactors but bubbles column was the poorest mixed because of lack of a well-defined bulk circulation of liquid. The configuration of the geometry of an airlift reactors was a significant part in controlling the mass transfer rate, it was notified by X. Lu (2000) who investigated the gas-liquid mass transfer between the modified square airlift loop reactors and the round airlift loop reactors and it was reported that when the superficial gas velocity is settled within the two extreme superficial velocity, the average k_{La} value in modified square airlift loop reactors is about 40% larger than that in round airlift loop reactors. Wongsuchoto (2003) also proved that k_{La} increased with superficial gas velocity (u_{sg}) but decreased with increasing cross-sectional area between the downcomer and riser (A_d/A_r) where the influence of number of holes in sparger on k_{La} was negligible. The summaries of work done on gas-liquid mass transfer shown in Table 2.2.

2.5 Bubble size distribution

There are several methods generally employed for the determination of interfacial area, for instance, the Danckwerts method which was based on the absorption of CO_2 in sodium or potassium carbonate–bicarbonate buffer solutions, dynamic gas disengagement method and photographic technique. In practice, bubble size is measured in terms of Sauter mean diameter, d_{B_s} , which refers to a diameter of a sphere with the same volume as the bubble:

$$d_{32} = \frac{\sum_{i=1}^N N_i d_i^3}{\sum_{i=1}^N N_i d_i^2} \quad (2.9)$$

where n_i is the bubble number having an equivalent sphere diameter, $d_{B,i}$ and d_B is the sphere diameter with the same volume as ellipsoidal bubble.

The entire range of ascending bubbles velocity can be tentatively divided into four regions (Treybal, 1980 and Kafarov, 1985):

- 1) $d_B < 0.7$ mm: The bubbles behave like solid particles and their velocities are governed by Stokes' law which is dependent on liquid properties and particle characteristics;
- 2) $0.7 \text{ mm} < d_B < 1.4$ mm: The bubbles retain the spherical shape but internal circulation appears, thus decreasing the stress on the interface. The ascent velocity exceeds the value calculated by Stokes' law;
- 3) $1.4 \text{ mm} < d_B < 6.0$ mm: The bubbles are no longer spherical and ascend in a zigzag manner. The resistance to their motion increases due to the hydrodynamic trail formation. A change in the bubble diameter does not have a significant effect on the ascent velocity;
- 4) $d_B > 6$ mm: The bubbles are bowl-shaped. The limiting ascent velocity increases with the bubble diameter.

Wongsuchoto et al. (2003) investigated the distribution of bubble size in annulus sparged airlift contactors (ALCs). The results showed that bubble sizes decreased along the axial distance in the riser. Moreover, bubble size can be related to the superficial gas velocity, for a low level of u_{sg} (< 0.01 m/s), most of the gas bubbles in the system had a diameter of 6.0–8.0 mm, for case $0.02 < u_{sg} < 0.04$ m/s, at least two dominant sizes of bubbles and at u_{sg} of 0.0296 m/s existed a relatively large bubble group with diameters of 7.0–8.0 mm and the other smaller group with diameters of 4.0–6.0 mm. At high u_{sg} (> 0.05 m/s), smaller bubbles with a diameter of 3.0–6.0 mm dominated the system and the group of large bubbles disappeared. Moreover, the higher ratio between the cross-sectional areas (A_d/A_r) could be operated with a higher level of u_{sg} . In most cases, the average bubble size tended to increase and narrow size distribution with an increased orifice number of sparger due to the high pressure in the sparger with a less number of orifices caused very large new-born bubble size and broke rapidly after leaving the orifice.

Table 2.1 Relative performance of external and internal airlift bioreactors

Parameter	Reactor	
	External Airlift Bioreactors	Internal Airlift Bioreactors
Mass Transfer Coefficient	Lower	Higher
Overall Gas holdup	Lower	Higher
Riser gas holdup	Lower	Higher
Downcomer gas holdup	Lower	Higher
Circulation Velocity	Higher	Lower
Circulation Time	Lower	Higher
Liquid Reynolds Number	Higher	Lower
Heat Transfer	Probably higher	Probably lower

ศูนย์วิทยทรัพยากร
จุฬาลงกรณ์มหาวิทยาลัย

Table 2.2 Literature review

Author (year)	Details	System	k_{La} (1/s)	Downcomer Gas holdup (-)	Overall Gas holdup (-)	U_{sg} (cm/s)	A_d/A_r (-)
Shing et al. (2003)	ILALC perforated ring sparger with 26 holes of 1 mm diameter	Air-Water	-	0.01-0.17	-	0.71-3.55	1.25
Choi et al. (1996)	ILALC perforated ring sparger with 30 holes of 2 mm diameter	Air-Water	0.003-0.072	-	0.038-0.165	1.00-8.00	1.00
Mehrnia et al. (2005)	ILALC perforated pipes sparger with 30 holes of 1 mm diameter	water-in-oil	0.0035-0.030	-	0.009-0.113	1.00-7.50	0.707
Korpijarvi et al. (1999)	ILALC perforated tube sparger of 0.09 mm diameter	Air-Water	0.047-0.251	0.015-0.122	-	1.00-13.20	0.14-1.69

Table 2.2 (cont.)

Author (year)	Details	System	k_{La} (1/s)	Downcomer Gas holdup (-)	Overall Gas holdup (-)	U_{sg} (cm/s)	A_d/A_r (-)
Chisti et al. (1994)	ILALC perforated ring sparger with with 38 holes of 1.5 mm diameter	Air-Water	-	0.05-0.23	-	2.00-17.00	1.8-7.7
Blazej et al. (2004)	ILALC Teflon plate sparger with with 25 holes of 1.0 mm diameter	Air-Water	-	0.009-0.055	-	0.50-3.00	0.95
Lu et al. (2000)	ILALC Teflon plate sparger with with 25 holes of 1.0 mm diameter	Air-Water	0.005-0.07	-	-	0.08-0.16	0.11-1.38
Wongsuchoto et al. (2003)	ILALC perforated ring sparger with with 14 holes of 1.0 mm diameter	Air-Water	0.008-0.052	-	0.01-0.12	0.59-7.37	0.07-1.00

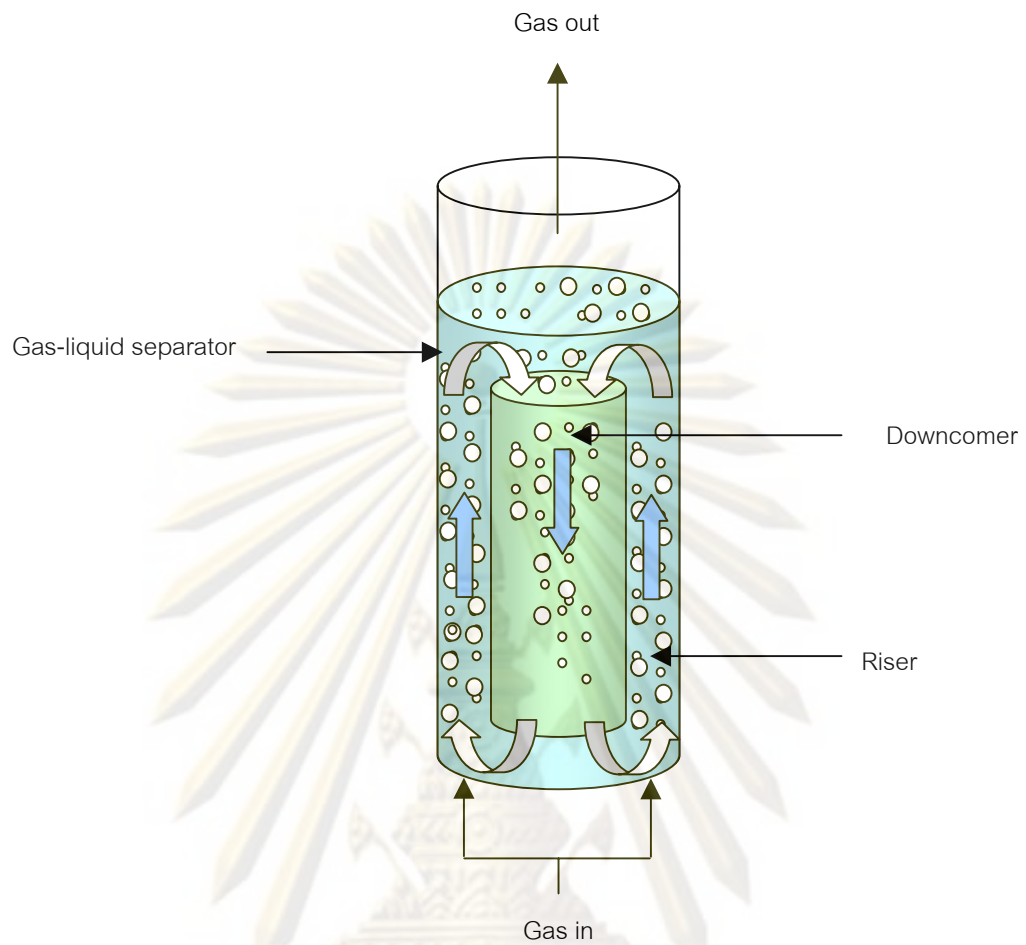


Figure 2.1 Schematic flow directions in airlift system

ศูนย์วิทยทรัพยากร
จุฬาลงกรณ์มหาวิทยาลัย

CHAPTER 3

Materials and Methods

3.1 Experimental setup

A schematic diagram of experimental system is illustrated in Figure 3.1. The airlift contactor (ALC) consists mainly of an outer cylinder and a draft tube. The outer cylinder has a diameter of 13.7 cm and the inner cylinder, or the draft tube has varied a diameter as detailed in Table 3.1. Draft tube is installed at the center of the column using the fixing arms. All parts are made from transparent acrylic plastic to allow visual observation and to record the movement of the color tracer for liquid velocity measurement. The ratio between downcomer and riser cross sectional areas (A_d/A_r) is altered by changing the draft tube diameter as detailed in Table 3.1. The annular sparger made from PVC is installed at the base of the column to introduce the gas phase into the ALC. The spargers with orifice numbers was fixed at 60. The bubble size distribution are measured using the digital video camera at three vertical locations as detailed in Table 3.2.

The manipulated parameters in this experiment include the sparger position, air flow rate, and the ratio between downcomer and riser cross sectional areas. The sparger position is basically the distance between the column base and the bottom of the draft tube and this will be varied from 0 to 12 cm. Air flow rate is controlled by a calibrated rotameter and this is varied in the range of superficial velocity from 4 to 10 cm/s. Table 3.3 summarizes the details of the experimental conditions employed in this work. A dissolved oxygen (DO) meter is used to measure the dissolved oxygen in the dispersion for the estimation of the mass transfer rate. In all experiments, tap water is used as liquid phase and the compressed air is used as gas phase. During the experiment, tap water is pumped into the column until the liquid level is 3 cm above the draft tube then air compressor pumps air into the system. The system is left running for a certain period of time to ensure a steady state operation before starting the measurement.

3.2 Experimental procedures

3.2.1 Measurement of bubble characteristics

The measurements of bubble size and distribution are performed only in the riser of the internal loop ALC using a general photographic technique method. The bubble sizes are measured at three sections of the column (parameter h in Table 3.2). The number of bubbles used in the measurement is more than 200 bubbles in each experiment. Bubble distortion due to the curvature of the outer column is compensated by comparing the measured size with the scale attached to the draft tube. The experimental steps are detailed as follows:

Procedure

1. Fill tap water into the concentric column until the liquid level (H_L) reaches 3 cm above the top of the draft tube
2. Turn on the lamp to illuminate the observation-desired point
3. Open valve to continuously disperse compressed air from an air compressor through the annular sparger to the column
4. Adjust superficial velocity (u_{sg}) to the desired value with calibrated rotameter
5. Record images of the bubbles at three different heights (h) as shown in Table 3.2
6. Calculate the bubble size using Equation 3.1
7. Repeat Steps 1 to 6 using other new geometric and/or operating parameters

3.2.2 Liquid velocity measurement

Liquid velocity is measured using the dye tracer method following the steps below.

Procedure

1. Fill tap water into the concentric column until the liquid level reaches the 3 cm level above the top of the draft tube
2. Open valve to continuously disperse compressed air from an air compressor through the sparger to the column

3. Inject dye tracer directly into the measuring port and measure the traveling time of the dye between any two vertical positions. The motion of the dye tracer is visually observed and a stopwatch is used to measure the time between the two positions.
4. Calculate riser and downcomer liquid velocity following Equations 3.2 and 3.3
5. Repeat Steps 1 to 4 using other new geometric and/or operating parameters

3.2.3 Mass transfer coefficient measurement

The overall volumetric mass transfer coefficient (k_La) is determined using the dynamic gassing method (Ruen-ngam et al., 2008). A dissolved oxygen (DO) meter is used to measure and record the changes in dissolved oxygen concentration in a batch of water. The experimental steps are detailed as follows:

Procedure

1. Fill tap water into the concentric column until the liquid level (H_L) is 3 cm above the top of the draft tube
2. Immerse the dissolved oxygen probe into the water in the column as shown in Figure 3.1 to measure the dissolved oxygen concentration in the water and ensure that all of the oxygen has been removed
3. Disperse nitrogen gas through the base of the contactor to the column for removing dissolved oxygen from the water in the column
4. Stop the nitrogen gas flow when the dissolved oxygen concentration reaches zero
5. Distribute compressed air from an air compressor continuously through the sparger into the column
6. Record the dissolved oxygen concentration with respect to time until the water is saturated with oxygen
7. Calculate the mass transfer coefficient (k_La) following Equation 3.4
8. Repeat Steps 1 to 6 using other new geometric and/or operating parameters

3.2.4 Gas holdup measurement

The overall gas holdup is determined by the volume expansion method. The gas holdup in the annular section is determined by the manometric method. The experimental steps are detailed as follows:

Procedure

1. Fill tap water into the concentric column until the liquid level (H_L) reached at 3 cm above the top of the draft tube
2. Open valve to continuously disperse compressed air from an air compressor through the sparger to the column
3. Adjust superficial velocity (u_{sg}) to the desired value by using calibrated rotameter
4. Read the liquid dispersion height (H_D) to evaluate the overall gas holdup in the airlift contactor
5. Measure the pressure difference between the two positions (ΔP) in the annular section by water manometer to evaluate the riser gas holdup. The calculation uses Equations 3.4 and 3.12. However, the gas holdup in the draft tube can not be measured directly, therefore the downcomer gas holdup is calculated following Equation 3.15.

3.3 Calculations

3.3.1 Bubble size calculation

For ellipsoidal bubbles, the major and minor axes of the bubble images are measured as shown in Figure 3.2. The equivalent diameter of a sphere with the same volume as the ellipsoidal bubble is calculated by (Ruen-ngam et al., 2008):

$$d_B = (p^2q)^{1/3} \quad (3.1)$$

3.3.2 Liquid velocity

The liquid velocities both in riser and downcomer are measured by the tracer injection method where the time at which the color uses for travelling between any two fixed positions is measured and used to calculate the velocity according to:

$$v_r = \frac{L_r}{t_r} \quad (3.2)$$

$$v_d = \frac{L_d}{t_d} \quad (3.3)$$

where v = liquid velocity [cm/s]
 L = distance between any two fixed position [cm]
 t = traveling time between two fixed positions [s]

3.3.3 Volumetric mass transfer coefficient calculation

The volumetric mass transfer coefficient (k_La) is determined by using the dynamic method. The time profile of the dissolved oxygen concentration in the solution is measured and recorded until the system reaches equilibrium. k_La can then be calculated from:

$$\ln \frac{(C^* - C_o)}{(C^* - C_L)} = k_Lat \quad (3.4)$$

where C^* = saturated oxygen concentration [mg / l]
 C_o = initial oxygen concentration [mg / l]

C_L = oxygen concentration in liquid phases [mg / l]

$k_L a$ = overall volumetric mass transfer coefficient [s^{-1}]

t = time [s]

3.3.4 Gas hold up calculations

1. Overall gas holdup

The overall gas holdup is determined by using a volume expansion technique. The expanded dispersion volume represents the gas volume in the system according to the following equation:

$$V_o = V_D - V_L \quad (3.5)$$

where V_o = expanded gas volume or overall gas volume [cm^3]

V_D = dispersed liquid volume [cm^3]

V_L = unaerated liquid volume [cm^3]

The fluid volume can be calculated from cross sectional area of the column (A) and fluid height (H) in these equations:

$$V = AH \quad (3.5a)$$

$$V_D = AH_D \quad (3.5b)$$

$$V_L = AH_L \quad (3.5c)$$

where A = cross sectional area of the column [cm^2]

H_D = dispersion height [cm]

H_L = unaerated liquid height [cm]

Moreover can calculate the overall gas hold up by:

$$V_o = \varepsilon_o AH_D \quad (3.5d)$$

where ε_o = gas fraction in the expanded fluid volume

From Equations (3.5), (3.5a), (3.5b), (3.5c) and (3.5d) we get:

$$\varepsilon_o AH_D = AH_D - AH_L \quad (3.6)$$

$$\varepsilon_o = \frac{(H_D - H_L)}{H_D} \quad (3.7)$$

where ε_o = overall gas holdup [-]

H_D = dispersed liquid height [cm]

H_L = unaerated liquid height [cm]

The unaerated liquid height and dispersion height can be measured from Section 3.2.2 and then the overall gas holdup can be calculated.

2. Riser gas holdup

For the annular sparged airlift contactor, the riser gas holdup is estimated by measuring the pressure difference between two measuring ports of the column.

Firstly,
$$\Delta P_{\text{column}} = \Delta P_{\text{manometer}} \quad (3.8)$$

$$\rho g \Delta H = \rho_L g \Delta Z \quad (3.9)$$

$$(\rho_L \varepsilon_L + \rho_g \varepsilon_g) g \Delta H = \rho_L g \Delta Z \quad (3.10)$$

Neglecting the wall friction loss and $\rho_L \gg \rho_g$, the gas holdup can be calculated from the following equations:

$$(\rho_L \varepsilon_L) g \Delta H = \rho_L g \Delta Z \quad (3.11)$$

$$\varepsilon_L = \frac{\rho_L g \Delta Z}{\rho_L g \Delta H} \quad (3.12)$$

since
$$\varepsilon_L = 1 - \varepsilon_G \quad (3.13)$$

so
$$1 - \varepsilon_G = \frac{\rho_L g \Delta Z}{\rho_L g \Delta H} \quad (3.14)$$

finally,
$$\varepsilon_r = 1 - \frac{\Delta P}{\rho_L g \Delta H} \quad (3.15)$$

where ΔP = pressure difference of defined liquid level in the column [$\text{g}/\text{cm} \cdot \text{s}^2$]

ΔH = height of defined liquid level in the column [cm]

ΔZ = height of liquid level in the manometer [cm]

ρ_g = gas density [g/cm^3]

ρ_L = liquid density [g/cm^3]

g = gravitational acceleration [cm/s^2]

3. Downcomer gas holdup

It is assumed that the gas holdup in the top section is approximately equal to in the riser. From this we can estimate the downcomer gas holdup from the overall and the riser gas holdup. The relationship between the gas holdups in the different parts of an airlift contactor can be written as:

$$\varepsilon_o = \frac{H_{dt}A_r\varepsilon_r + H_{dt}A_d\varepsilon_d + (H_D - H_{dt})(A_r + A_d)\varepsilon_t}{H_D(A_r + A_d)} \quad (3.16)$$

substituting $\varepsilon_t = \varepsilon_r$ into Equation 3.16 yield:

$$\varepsilon_o = \frac{H_{dt}A_d\varepsilon_d + (H_D A_d + H_D A_r - H_{dt} A_d)\varepsilon_r}{H_D(A_r + A_d)} \quad (3.17)$$

or

$$\varepsilon_d = \frac{\varepsilon_o H_D(A_r + A_d) - H_D A_d + H_D A_r - H_{dt} A_d}{H_D(A_r + A_d)} \varepsilon_r \quad (3.18)$$

where ε_o = overall gas hold up [-]

ε_r = gas holdup in riser [-]

ε_d = gas holdup in downcomer [-]

A_d = cross sectional area of downcomer [cm²]

A_r = cross sectional area of riser [cm²]

Table 3.1 Dimensions of draft tubes

Draft Tube	D_d [cm]	D_r [cm]	A_d/A_r [-]
1	9.00	9.77	0.90
2	5.40	12.0032	0.20
3	10.12	8.54	1.40

Table 3.2 Locations of digital video camera for bubble size measurement (parameters as shown in Fig. 3.1)

Section	Height from the bottom of the draft tube [cm]
Top section (h_1)	90
Middle section (h_2)	50
Bottom section (h_3)	10

Table 3.3 Specification of ALC used in this work. (cm)

Key	A_d/A_r	Sparger position
ALC-1	0.20	0
ALC-2	0.90	0
ALC-3	1.40	0
ALC-4	1.40	6
ALC-5	1.40	12

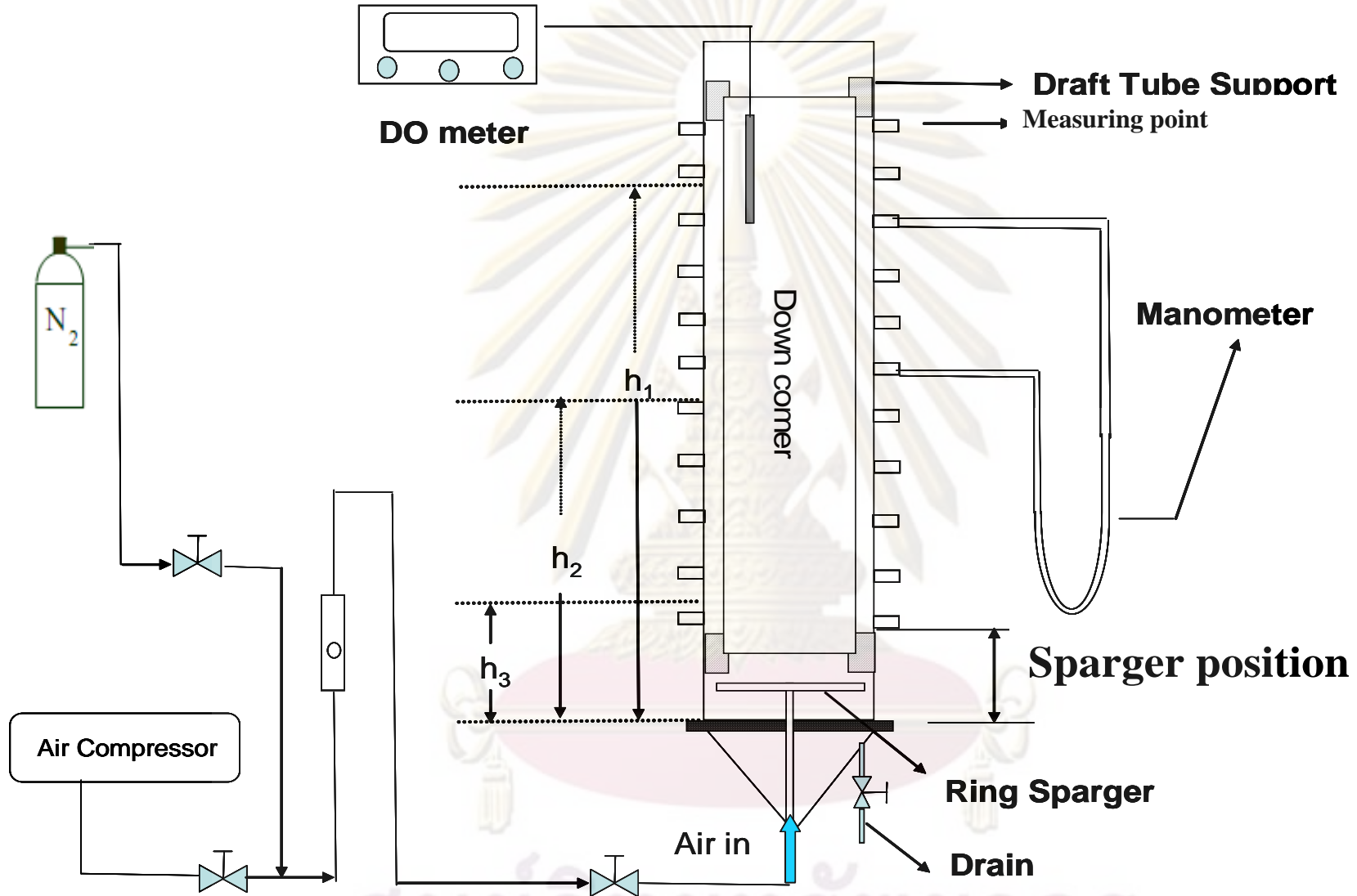


Figure 3.1 Schematic diagram of concentric internal loop airlift contactor employed in this work

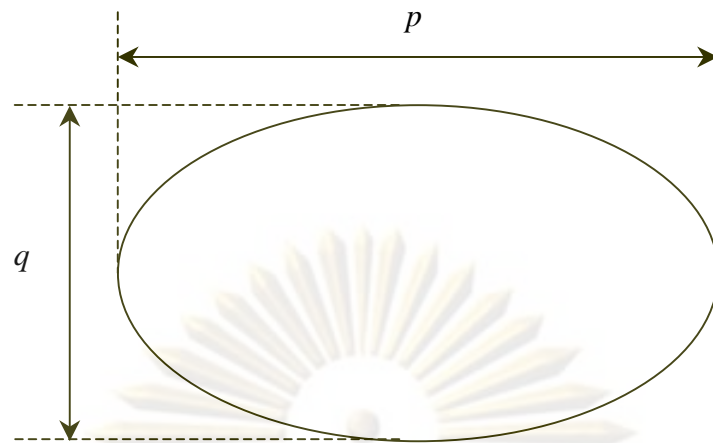


Figure 3.2 Major and minor axes of bubble images



ศูนย์วิทยทรัพยากร
จุฬาลงกรณ์มหาวิทยาลัย

CHAPTER 4

Results and Discussion

4.1 Error compensation in photographic technique

The measurement of bubble diameter in this study was taken along axial direction. The radial distribution of bubble size was not observed as the annulus of the employed ALCs had a rather small cross sectional area where the distance between inner and outer columns was only 0.01-0.05 cm which was approximately in the same order of magnitude with the bubble. This did not allow precise measurement of bubble sizes along radial direction. The measured sizes of bubbles were subject to error due to the curvature of the column surface. To account for this error, an object with a known size was placed along radial direction in the column and its picture was taken for size compensation. The error was then calculated and used as a correction factor for subsequent measurement. Note that the error due to the curvature of the column surface was approximately $\pm 15\%$. [Figure 4.1](#) is an example of photographs of bubbles obtained from this measurement technique. (Wongsuchoto 2003)

4.2 Bubble size distribution as a function of sparger position

[Figures 4.3-4.7](#) illustrate the effect of sparger position on bubble size distribution at various superficial gas velocities in the airlift with the ratio between riser and downcomer cross-sectional area (A_d/A_r) fixed at 1.4. The sparger was attached to the bottom of the contactor and the space between the sparger and the bottom of the column was varied from 0 to 12 cm (as detailed in Table 3.3).

The bubble size distribution curves in the riser as illustrated in [Figures 4.3-4.7](#) clearly show that a narrow size distribution exists for most systems. For cases where the sparger was far from base of the reactor (ALC-4 and ALC-5), majority of bubbles in these ALC have larger size than those in ALC-3 where the sparger was located at the base of reactor. At the lowest sparger position (ALC-3), there existed a group of small bubbles in the reactor. [Figure 4.8](#) shows the axial distribution of the average bubble size in ALC-1 to ALC-5. It was demonstrated that, at low sparger position (ALC-3 and ALC-4), the average bubble sizes of ALC at all height levels were smaller than those in the system with higher sparger position (ALC-5). There was a

potential that bubble breakage took place in the system at this low sparger position. In brief, the bubble size became larger at higher sparger position (d_{Bs} : ALC-5 > ALC-4 > ALC-3).

To describe the phenomena, the finding could be analyzed as follows. In airlift systems, the fluid circulates upwards in riser and downwards in downcomer before re-entering the riser at the bottom of the column. Therefore, if the sparger position was lower than the connecting point between rise and downcomer, this flow pattern pushed the bubbles towards the wall (see [Figure 4.2](#) for a better description). In such cases, small bubbles could be generated from the collision between the bubble and the wall. On the other hand, if the sparger was located above the connecting tube, the bubbles would not be dragged against the wall and a lower level of bubble breakage was observed. To put it more simply, the airlift with lower sparger position provided smaller Sauter mean bubble diameter than that with higher sparger position.

On the other hand, in ALC-4 and ALC-5 where the spargers were located at 6 and 12 cm above base of column respectively, this riser-downcomer connecting point was located below the sparger, therefore the flow pattern did not have significant impact on the movement of the bubbles, and the bubbles flowed upwards undisturbed. This lowered the chance of bubble breakage resulting in a larger bubble size.

4.3 Bubble size distribution as a function of superficial gas velocity

[Figures 4.3-4.7](#) illustrate the bubble size distribution curves from three vertical sections of ALC-1 to ALC-5. This revealed that there was only one main bubble size in the system and the size distribution function was slightly changed in this work. Bubble size did not seem to change further when superficial velocity became higher than 0.08 m/s. As a general trend, bubble size was quite large, in range of 5-7 mm at low superficial gas velocity ($u_{sg} < 0.08$ m/s), and became smaller, in a range of 3-4 mm, at high superficial gas velocity (u_{sg} between 0.08 and 0.10 m/s).

At a low level of u_{sg} (< 0.06 m/s) as shown in [Figure 4.9](#), the Sauter mean bubble diameter tended to increase with decreasing gas throughput. As u_{sg} is raised above 0.08 m/s, on account of an increase in the frequency of bubble coalescence, the bubble size in the system became smaller with a diameter range of 4.0-3.0 mm as shown in the distribution curve in [Figures 4.3-4.7](#). Literature indicates that an increase in u_{sg} led to high energy dissipation and turbulent eddies which caused more bubble

breakage. Fundamentally, an increase in u_{sg} led to high liquid velocity and this might enhance turbulent intensity. However, a further increase in gas throughput (>0.08 m/s) did not seem to further influence bubble size. This finding agreed with the literature by Wongsuchoto et al. (2003) who studied the bubble size distribution in ALC with perforated ring sparger working in gas-liquid system. They stated that this might be due to the stability of small bubble against the breakage mechanism.

4.4 Average bubble size as a function of ratio between downcomer and riser cross-sectional area

To investigate the effect of the ratio between downcomer and riser cross-sectional area (A_d/A_r), the experiment was conducted in the airlift contactor with the sparger fixed at the base of the column (0 cm). Three different A_d/A_r , i.e. 0.2 (ALC-1), 0.9 (ALC-2), and 1.4 (ALC-3) were used. Figure 4.9 illustrates that, at low superficial gas velocity, no significant differences in Sauter mean bubble diameter were observed among the three systems. Camarasa et al. (1999) reported that the homogenous regime (bubbly flow) occurred at low gas throughput where bubbles moved uniformly and coalescence and break up could be neglected. Therefore the bubble size remained constant and equaled the original size from the sparger. In contrast, at higher superficial gas velocity, A_d/A_r seemed to play a more important role on bubble size. The bubble size was found to be smaller with an increasing draft tube size (smaller riser cross-sectional area). This might be because, in the system with smaller riser area, turbulence in the system was higher than those with larger riser area. It was possible that liquid moved with faster velocity in the system with small riser (small A_r) and the chance of bubble being broken to small bubbles were formed.

4.5 Axial average bubble size in airlift contactor

Figure 4.10 demonstrates that the Sauter mean bubble diameter at the bottom section of the airlift column was found to be larger than those in other sections particularly at high u_{sg} . This observation was not obvious at low u_{sg} as the system was still in bubbly flow condition. At high u_{sg} , it was observed that the bubble size decreased as a function of increasing column height. This suggested that there was a higher level of turbulence in the top and middle sections which could break the bubble along the height of the system. This result is consistent with the reports of Colella et

al., (1999), Wongsuchoto et al., (2003) and Ruen-ngam et al., (2008) who measured bubble size as a function of height in bubble column and concluded that the relative frequency of the small bubbles increased with increasing distance up from sparger. At a higher u_{sg} , the small bubbles did not seem to break and the Sauter mean bubble size was independent of column height.

4.6 Overall volumetric mass transfer coefficient (k_La) in airlift contactors

In gas–liquid contactors, the interfacial mass transfer from gas to liquid is one of the most important goals, and the extent of mass transfer is typically indicated using the overall volumetric mass transfer coefficient (k_La) (Eq. 3.4). The relationships between the overall volumetric mass transfer coefficients (k_La) in the ALC with various parameters as shown in Figure 4.11 revealed that k_La increased with an increase in u_{sg} . Similar to the gas holdup, lowering sparger position could enhance the overall volumetric mass transfer coefficient. As stated earlier, lowering sparger position resulted in a smaller average bubble size, hence, more surface area for gas-liquid mass transfer was available leading to a higher gas-liquid mass transfer rate.

Figure 4.11 also describes the effect of A_d/A_r on k_La (ALC-1, ALC-2 and ALC-3). It should be noted that the ALC with larger A_d/A_r seemed to accelerate the liquid circulating velocity (Fig. 4.12), therefore, reducing the overall gas holdup (Fig. 4.13). On the other hand, as stated in Section 4.4, the Sauter mean bubble diameter was small in the system with larger A_d/A_r . (Fig. 4.9), and this could enhance the specific interfacial area. Normally, the specific interfacial area will depend on two parameters: gas holdup and bubble size. The results in Figures 4.9, 4.13-4.14 demonstrated clearly that, in this case, the effect of gas holdup was far more significant than bubble size in dictating the specific surface area. Figures 4.11 illustrates further that k_La also depended more notably on the specific interfacial area (and gas holdup) than other parameters.

To further investigate the gas-liquid mass transfer performance, it is noted that k_La composes of two main parameters, i.e. “ k_L ” (overall mass transfer coefficient), and “ a ” (specific interfacial area). Generally k_L is a function of turbulence, liquid

properties and bubble size. The specific interfacial area (a) can be calculated from the Sauter mean diameter, d_{Bs} , and the gas holdup, ε_g , as follows:

$$a = \frac{6\varepsilon_G}{(1-\varepsilon_G)d_B} \quad (4.1)$$

Sauter mean diameter is further defined as:

$$d_{Bs} = \frac{\sum_i n_i d_{B_i}^3}{\sum_i n_i d_{B_i}^2} \quad (4.2)$$

where n_i is the occurrence frequency number of the sphere bubble diameter, d_{B_i} . [Figure 4.13](#) demonstrates that the overall gas holdup, $\varepsilon_{g,o}$, was higher at lower sparger position. This was simply because sparger installed at lower position generated smaller bubbles which then moved at lower speed, increasing the residence time and holdup in the system. As stated earlier in Section 4.2, the Sauter mean diameter was greater in the system with higher position of sparger compared with the lower ones. This could be due to the reason that when bubbles were dispersed from the lowest sparger position, they were pushed against the wall by the recirculating fluid from the downcomer, and thus the collision between bubble and wall of reactor occurred leading to bubble breakage.

The overall volumetric mass transfer coefficient $(k_L a)_T$ could be calculated from the sum of the mass transfer rates in riser and downcomer sections as follows:

$$(k_L a)_T = \frac{(k_L a)_r V_{Lr} + (k_L a)_d V_{Ld}}{V_{LT}} \quad (4.3)$$

where V_{Lr} is the volume of liquid in riser, V_{Ld} the volume of liquid in downcomer and V_{LT} the volume of total liquid. $(k_L a)_r$ and $(k_L a)_d$ were obtained from $k_{L,r}$ multiplied by a_r and $k_{L,d}$ multiplied by a_d . The parameter $k_L a$ calculated from this equation was compared relatively well with a deviation range of $\pm 20\%$ with $k_L a$ from the experiment as shown in [Figure 4.15](#).

The most important characteristics affecting the mass transfer coefficient (k_L) between the gas-liquid phases are physical properties of the solution and the size of bubbles (d_{Bs}), or their distribution (Gracia-Ochoa et al., 2004). Several empirical and theoretical correlations for the determination of k_L for various systems are given and summarized in Skelland, 1974, Welty 1984, Stanley, 1998, and Painmanakul et. al., 2005. Equation (4.4) is often used to estimate k_L .

$$Sh = a + b Gr^c Sc^d + e Re^f Sc^h \quad (4.4)$$

The dimensionless relationship between Sherwood numbers (Sh), Schmidt number (Sc), Grashof number (Gr) and Reynolds number (Re) can be written as:

$$Sh = \frac{k_L d_{Bs}}{D_L} \quad (4.5)$$

$$Gr = \frac{d_{Bs}^3 \rho_l \Delta \rho g}{\mu_l^2} \quad (4.6)$$

$$Re = \frac{d_{Bs} v_s \rho_l}{\mu_l} \quad (4.7)$$

Generally, Grashof number (Gr) represents mass transfer by free convection or the acceleration of free fall whereas Reynolds number (Re) is for mass transfer by forced convection. The parameters d_{Bs} and v_s in the calculation of Reynolds number are the Sauter mean bubble diameter and slip velocity. The Sauter mean bubble diameter riser (d_{Bsr}) can be calculated from the terminal riser velocity of single bubble, u_∞ , which is determined by its size, interfacial tension, the density and viscosity of the surrounding liquid. (Bozzana et al., 2001) Information on bubble sizes is required for the estimation of the slip velocity of the gas bubbles in the system using the following equation (Marrucci, 1965; Wallis, 1969):

$$v_{sr} = \frac{u_\infty}{(1 - \varepsilon_{Gr})} \quad (4.8)$$

where u_∞ is the bubble's terminal riser velocity, physically, the velocity depends on five parameters (Mario et al., 2008)

$$u_\infty = u_\infty(g, d_{Bs}, \rho, \mu, \sigma) \quad (4.9)$$

which can be calculated using the correlation proposed by Jamialahmadi et al., 1994,

$$u_\infty = \frac{\frac{1}{18} \frac{\rho_L - \rho_G}{\mu_L} g d_{Bs}^2 \left(\frac{3\mu_L + 3\mu_G}{2\mu_L + 3\mu_G} \right) \sqrt{\frac{2\sigma_L}{d_{Bs}(\rho_L + \rho_G)} + \frac{g d_{Bs}}{2}}}{\sqrt{\left[\frac{1}{18} \frac{\rho_L - \rho_G}{\mu_L} g d_{Bs}^2 \left(\frac{3\mu_L + 3\mu_G}{2\mu_L + 3\mu_G} \right) \right]^2 + \frac{2\sigma_L}{d_{Bs}(\rho_L - \rho_G)} + \frac{g d_{Bs}}{2}}} \quad (4.10)$$

where g is the acceleration due to gravity, d_{Bs} the Sauter mean diameter, μ the dynamic viscosity (L for liquid and G for gas), σ_L the surface tension, ρ_L the density of liquid and ρ_G the density of gas.

As the limitation of photographic technique, bubble size in downcomer was not known and the determination of slip velocity in downcomer was not possible.

Therefore, the Sauter mean bubble diameter downcomer (d_{Bsd}) was estimated from experimental data on liquid velocity in downcomer (u_{Ld}) using the Levich equation:

$$d_{Bsd} = \frac{1.8}{g} \left(\frac{u_{Ld}}{2} \right)^2 \quad (4.11)$$

It was assumed further that there was no variation of bubble size along the radial and axial directions in downcomer. Therefore,

$$d_{Bsd} = d_{Bd} \quad (4.12)$$

The specific interfacial area in downcomer (a_{Ld}) is calculated from the substitution of d_{Bsd} from Equation 4.12 and $\varepsilon_{g,d}$ could be calculated from Equation 4.13. Therefore, a_{Ld} can be calculated by substituting d_{Bsd} and $\varepsilon_{g,d}$ into Equation 4.1.

$$\varepsilon_{g,o} = \frac{A_r \varepsilon_r + A_d \varepsilon_d}{A_r + A_d} \quad (4.13)$$

The liquid velocity in downcomer (u_{Ld}) in Equation 4.11 can be estimated from the continuity equation (Eq. 4.14) for the case where the liquid mass flow in downcomer was equal to that in riser, and local internal liquid circulation was assumed not to exist (Wongsuchoto et al. 2004). It should be noted that the liquid velocity in riser (u_{Lr}) was obtained from the measurement with the color tracer technique.

$$u_{Ld} A_d (1 - \varepsilon_{g,d}) = u_{Lr} A_r (1 - \varepsilon_{g,r}) \quad (4.14)$$

Figure 4.15 illustrates the comparison between the predicted $k_L a$ from Equation 4.3 and the experimental value which operated in airlift contactors. The parameters $a-e$ in Equation 4.4 were equal to 0.5, 1.07 and 0.51. These results are close to those proposed from Wongsuchoto et al., 2003 and Ruen-ngam et al., 2008 as shown in Table 4.1. (Note that these parameters were obtained from the solver function in the MS Excel 97 where the objective was a minimal error between experimental and simulation data of $k_L a$). Equation 4.4 can finally be reduced to:

$$Sh = 0.5 + 1.07 Gr^{0.51} \quad (4.15)$$

Equation 4.15 indicates that when the coefficient “ d ” equals zero, Re disappears, which means that forced convection has no effect on the mass transfer. This finding reveals that the mass transfer in the ALC employed in this work depended primarily on the natural convection, and not the force convection.

4.7 Empirical models for the prediction of the Sauter mean bubble diameter of various parameters

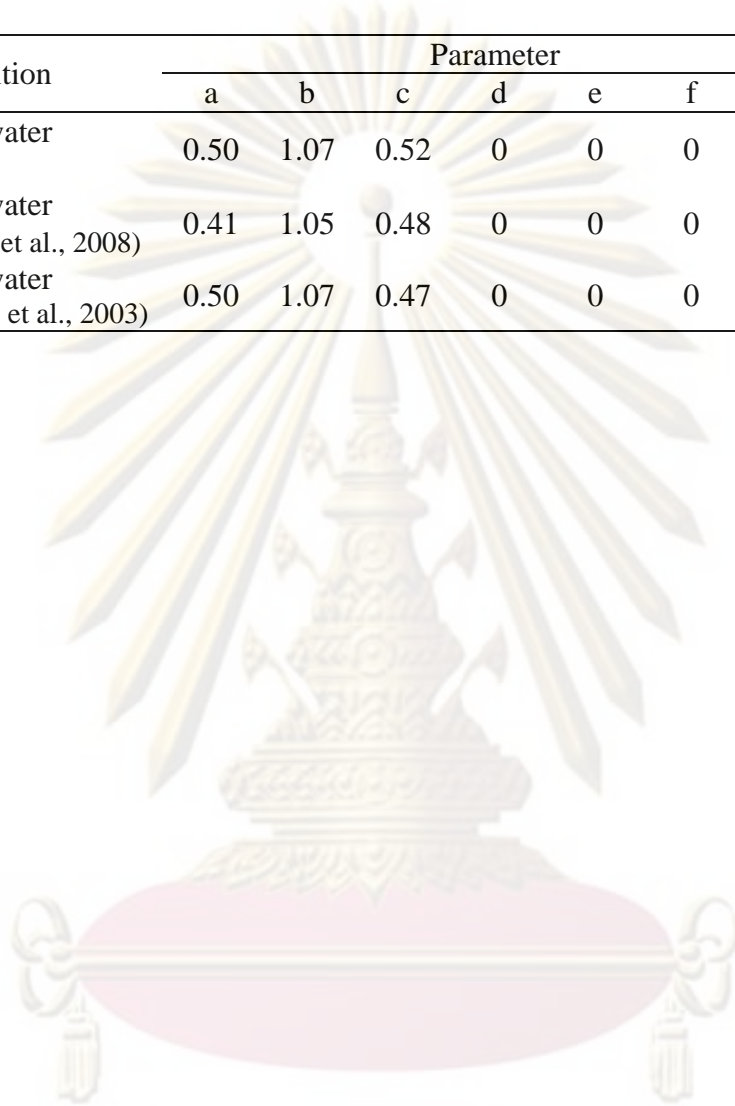
The three parameters were investigated for the effect of the Sauter mean diameter as shown above, three parameters including, sparger position, superficial liquid velocity and ration between downcomer and riser cross-sectional area. The following empirical equation was used for estimating the Sauter mean diameter in the internal airlift system for tap water as shown:

$$d_{Bs} = 0.006(u_{sg}^{-0.354})(A_d/A_r)^{-0.068}(\text{Sparger Position}+113.633)^{1.222} \quad (4.16)$$

The accuracy of empirical models proposed in this work was verified with the experimental data with the deviation range of $\pm 10\%$ (as displayed in [Figure 4.16](#)).

Table 4.1 Parameters from the initial establishment of k_L correlation in Equation 4.4 $Sh = a + bGr^c Sc^d + e Re^f Sc^h$

Condition	Parameter							R^2
	a	b	c	d	e	f	h	
Tap water	0.50	1.07	0.52	0	0	0	0	0.89
Tap water (Ruen-ngam et al., 2008)	0.41	1.05	0.48	0	0	0	0	0.91
Tap water (Wongsuchoto et al., 2003)	0.50	1.07	0.47	0	0	0	0	0.92



ศูนย์วิทยทรัพยากร
จุฬาลงกรณ์มหาวิทยาลัย



Figure 4.1 Example photograph of bubbles obtained from the photographic measurement technique

ศูนย์วิทยทรัพยากร
จุฬาลงกรณ์มหาวิทยาลัย

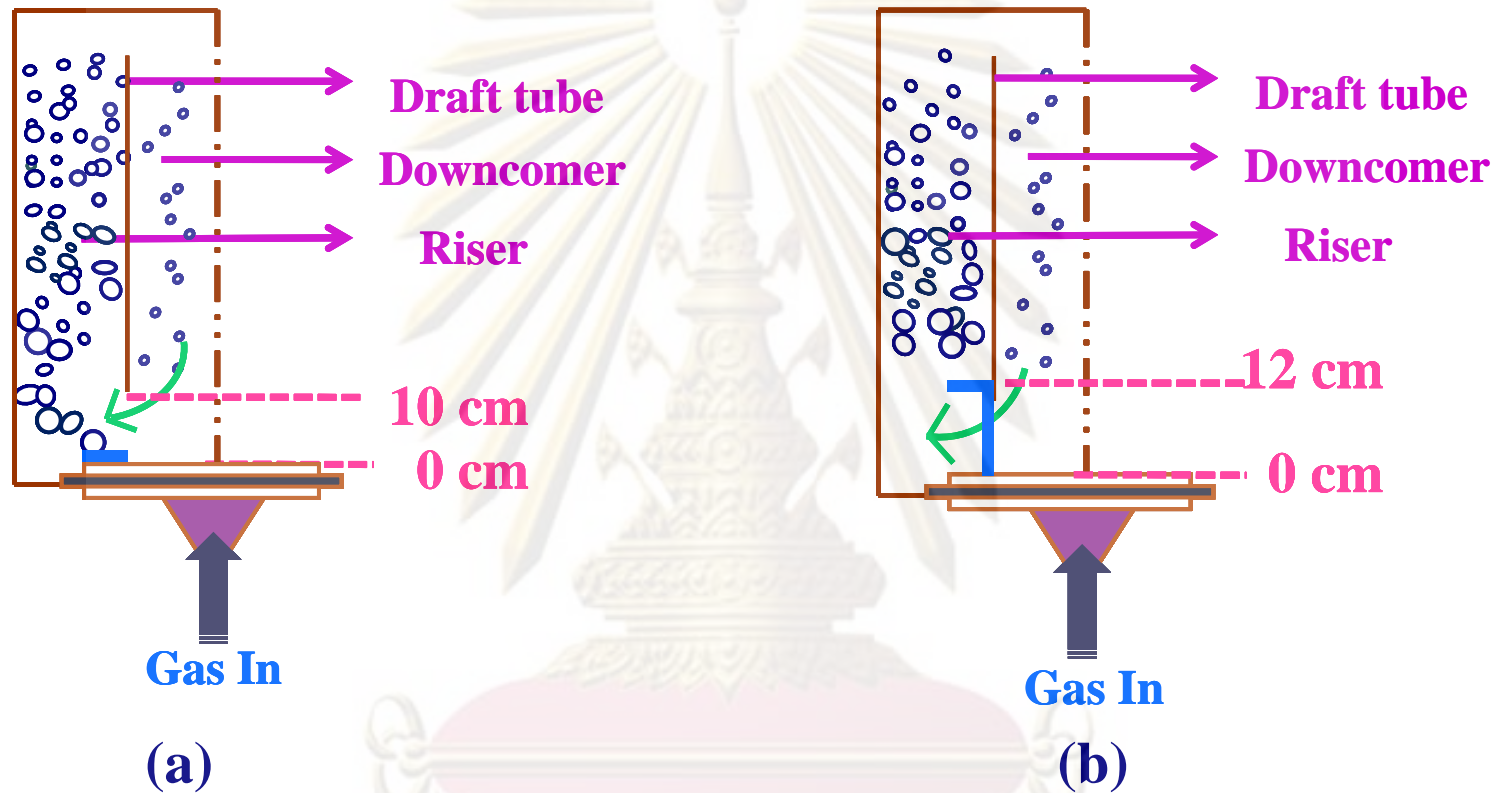


Figure 4.2 Effect of sparger position on gas distribution in airlifts
 (a) Distribution of gas when sparger is located at 0 and 6 cm above the base of the reactor
 (b) Distribution of gas when sparger is located 12 cm above the base the reactor

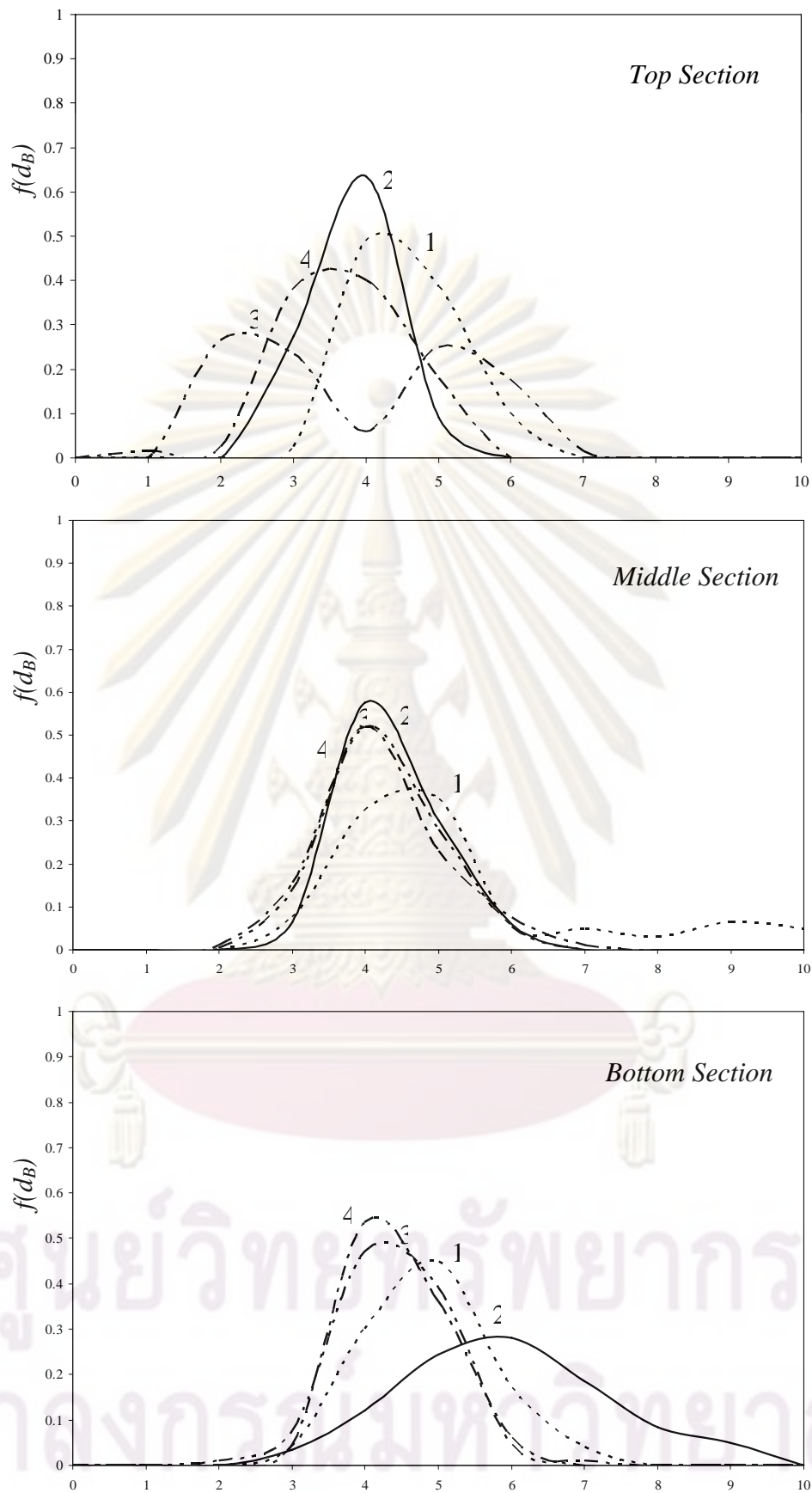


Figure 4.3 Frequency distribution of bubble sizes in ALC-1: (1) $u_{sg} = 0.04$ m/s (2) $u_{sg} = 0.06$ m/s (3) $u_{sg} = 0.06$ m/s and (4) $u_{sg} = 0.10$ m/s

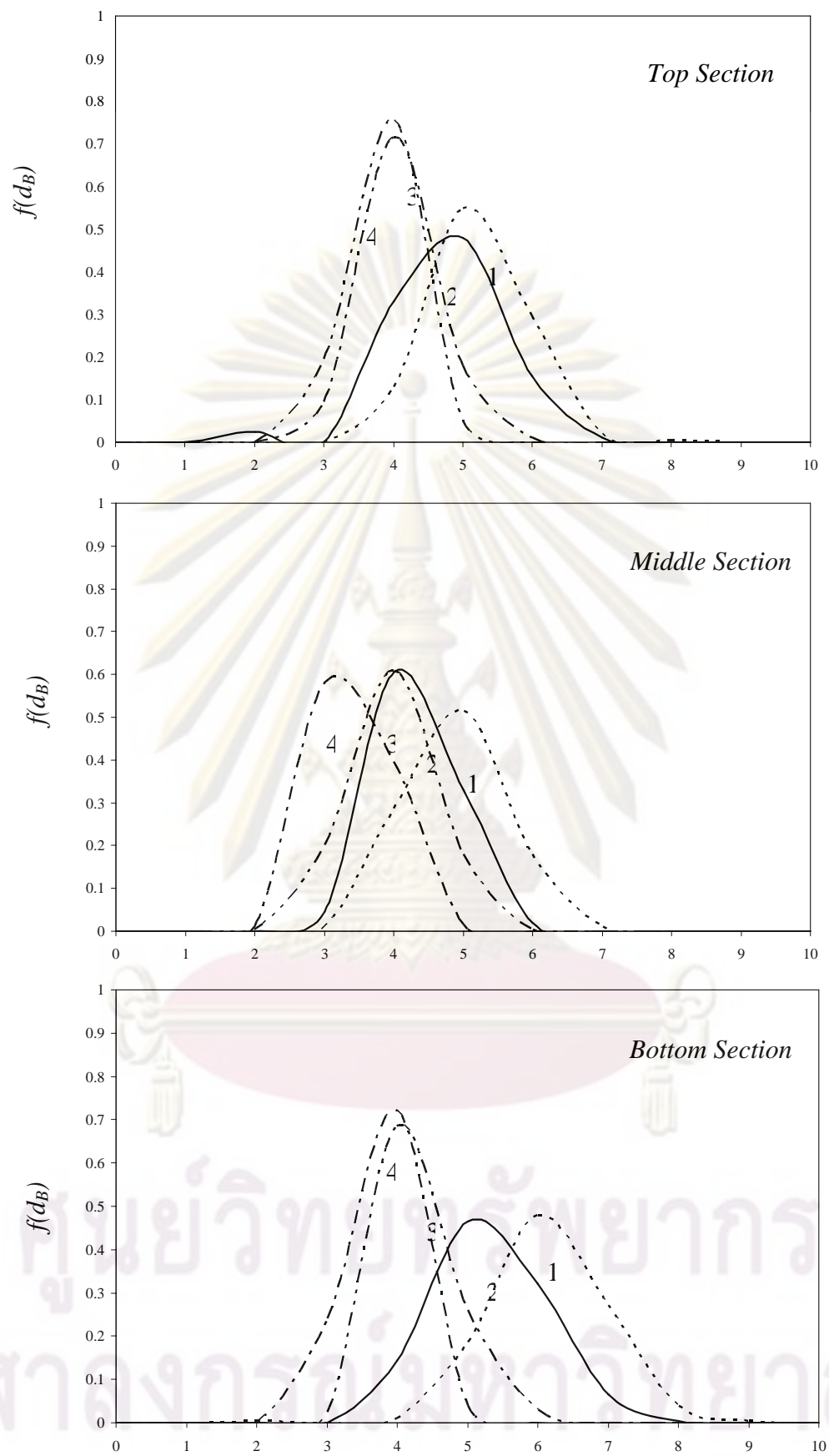


Figure 4.4 Frequency distribution of bubble sizes in ALC-2: (1) $u_{sg} = 0.04\text{m/s}$ (2) $u_{sg} = 0.06\text{ m/s}$ (3) $u_{sg} = 0.06\text{ m/s}$ and (4) $u_{sg} = 0.10\text{ m/s}$

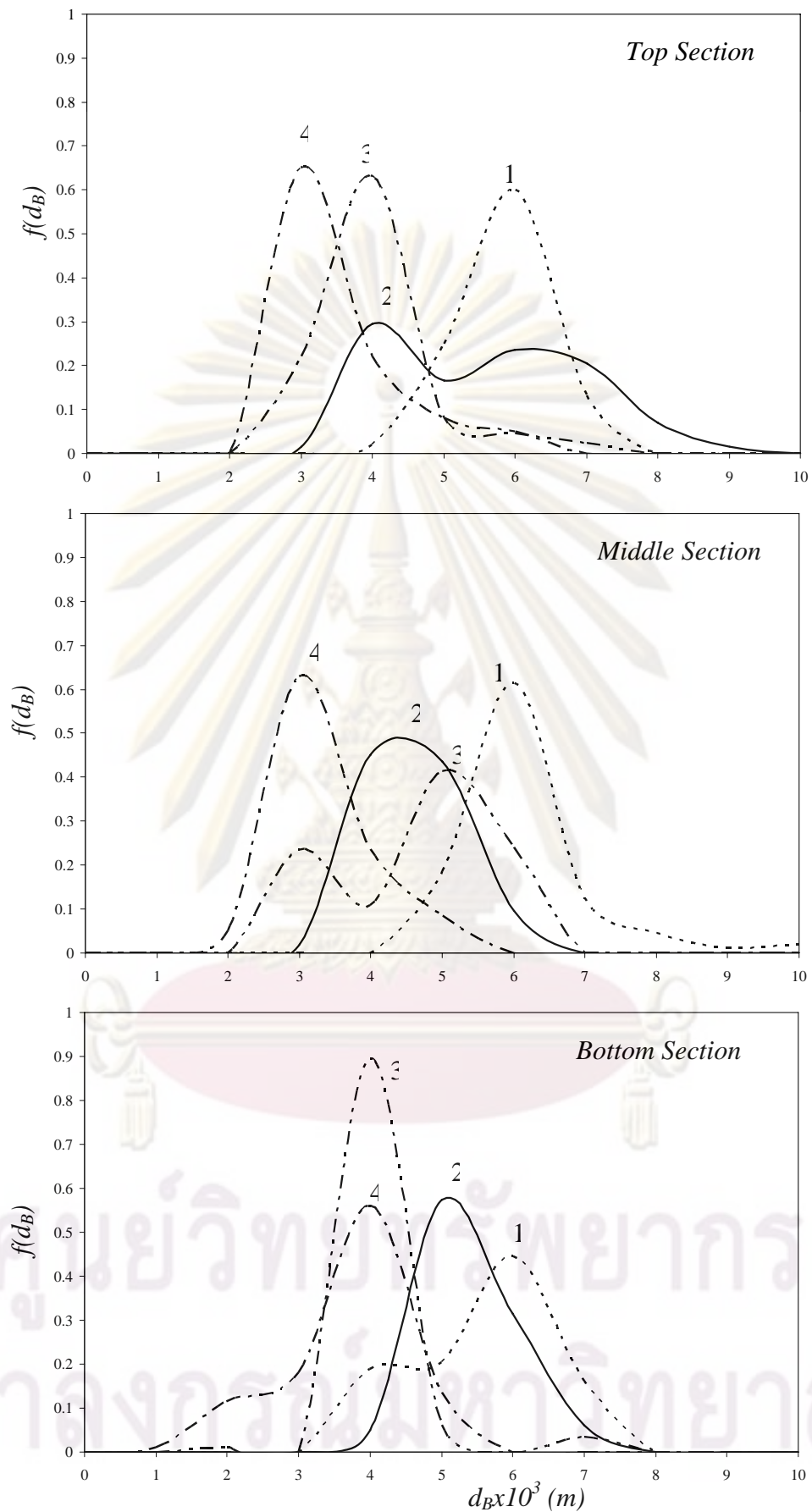


Figure 4.5 Frequency distribution of bubble sizes in ALC-3: (1) $u_{sg} = 0.04$ m/s (2) $u_{sg} = 0.06$ m/s (3) $u_{sg} = 0.06$ m/s and (4) $u_{sg} = 0.10$ m/s

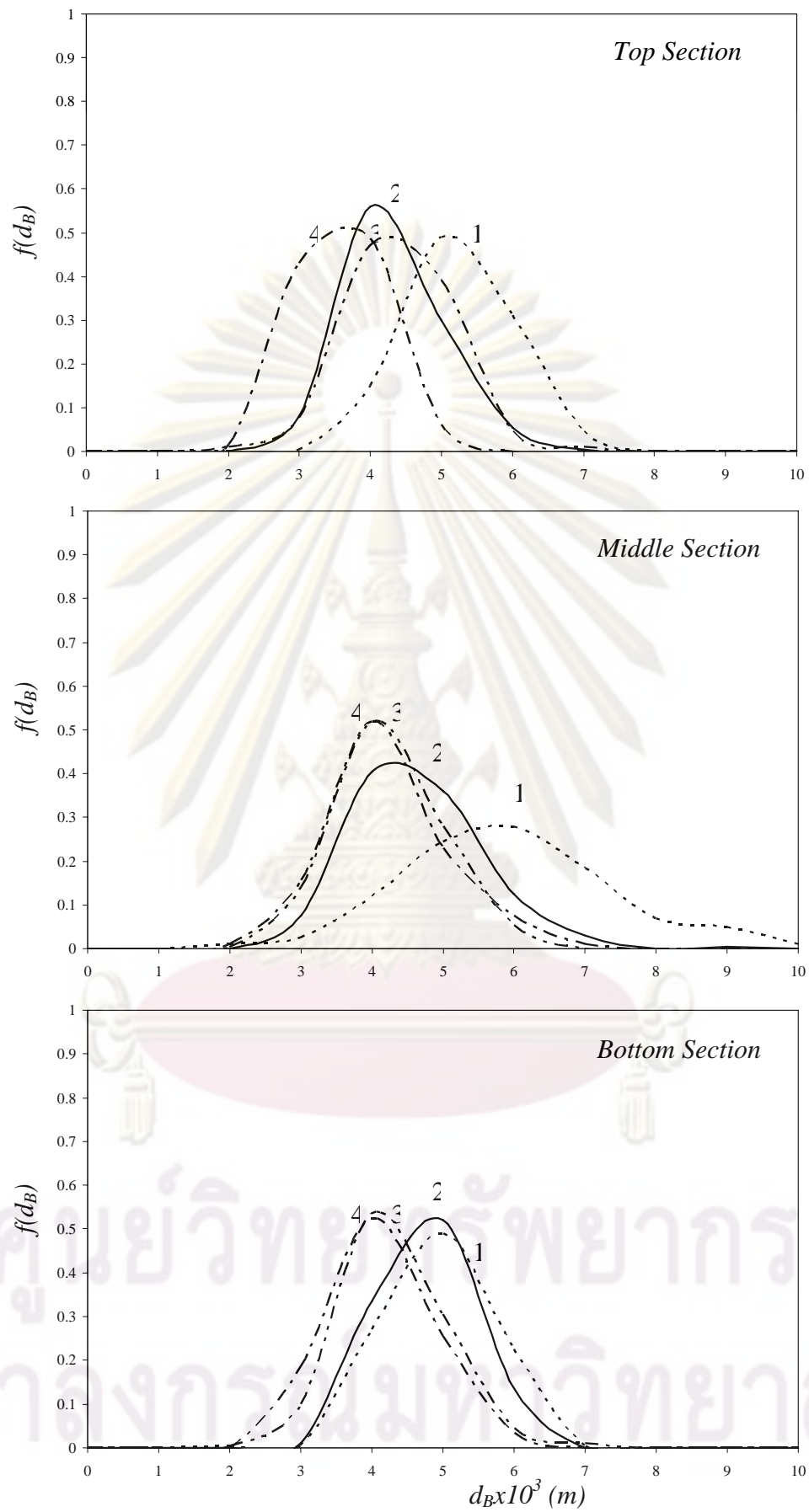


Figure 4.6 Frequency distribution of bubble sizes in ALC-4: (1) $u_{sg} = 0.04$ m/s (2) $u_{sg} = 0.06$ m/s (3) $u_{sg} = 0.06$ m/s and (4) $u_{sg} = 0.10$ m/s

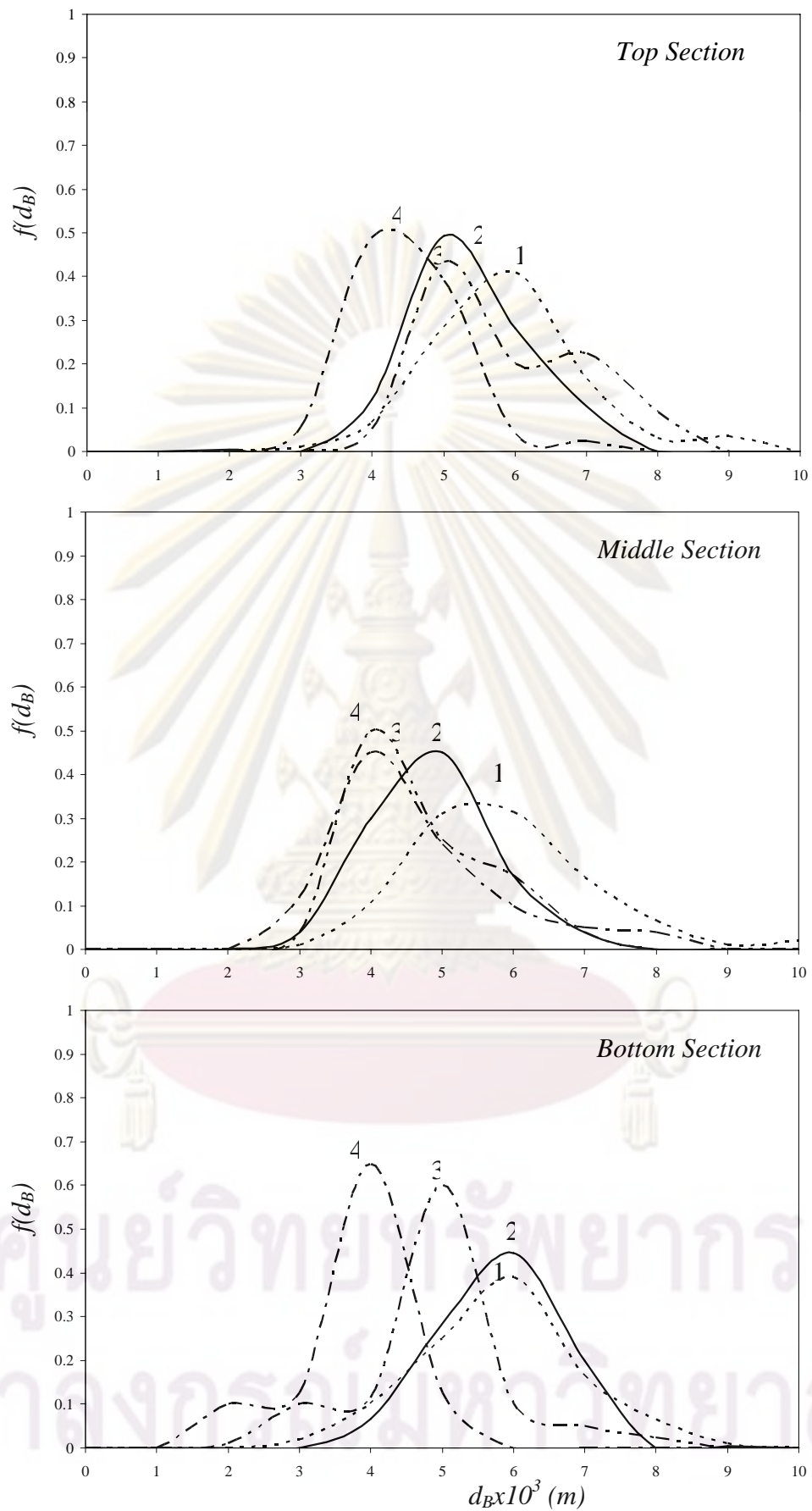


Figure 4.7 Frequency distribution of bubble sizes in ALC-5: (1) $u_{sg} = 0.04$ m/s (2) $u_{sg} = 0.06$ m/s (3) $u_{sg} = 0.06$ m/s and (4) $u_{sg} = 0.10$ m/s

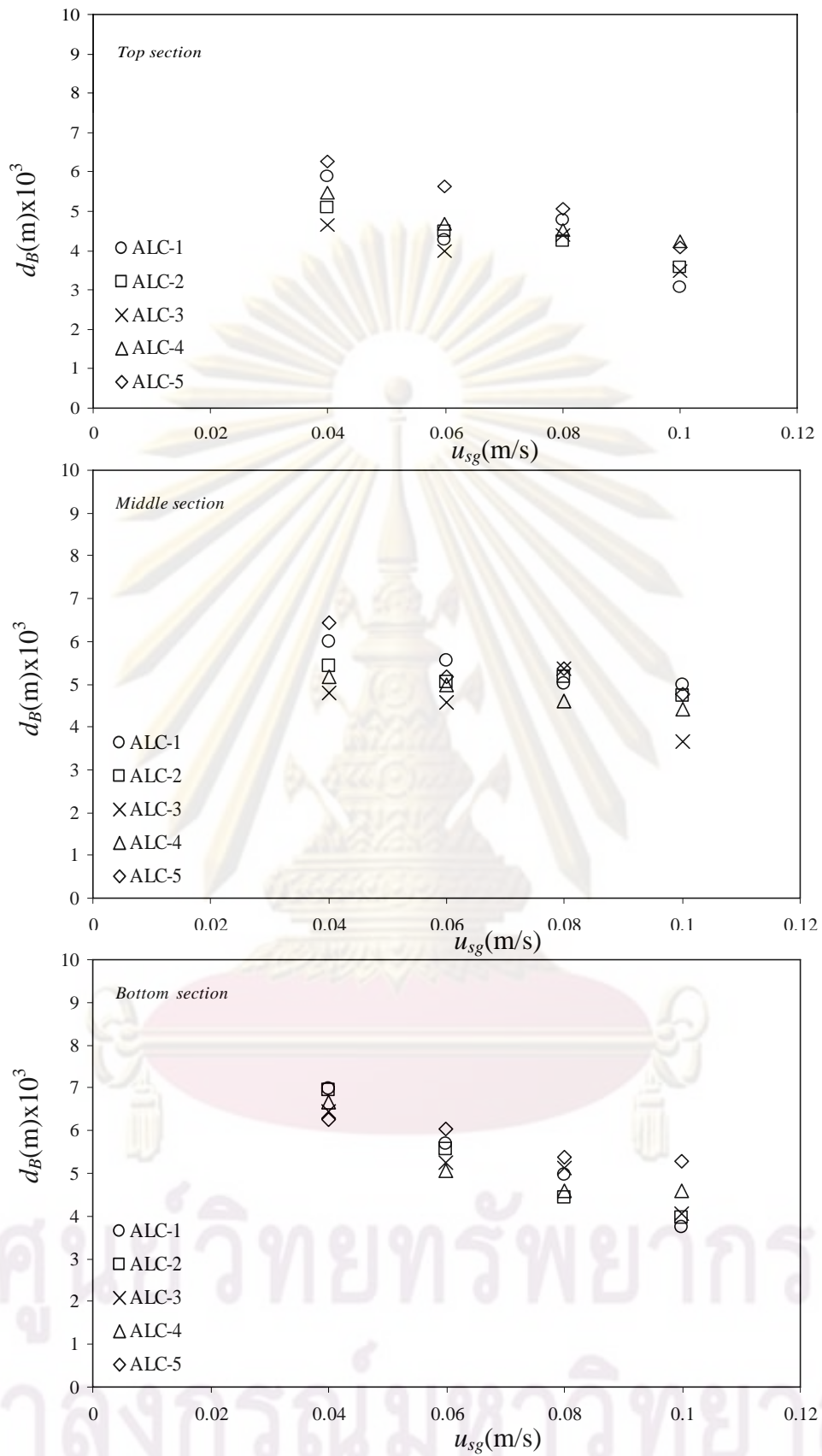


Figure 4.8 Relationship between average bubble diameter (d_B) and superficial gas velocity (u_{sg}) along axial location

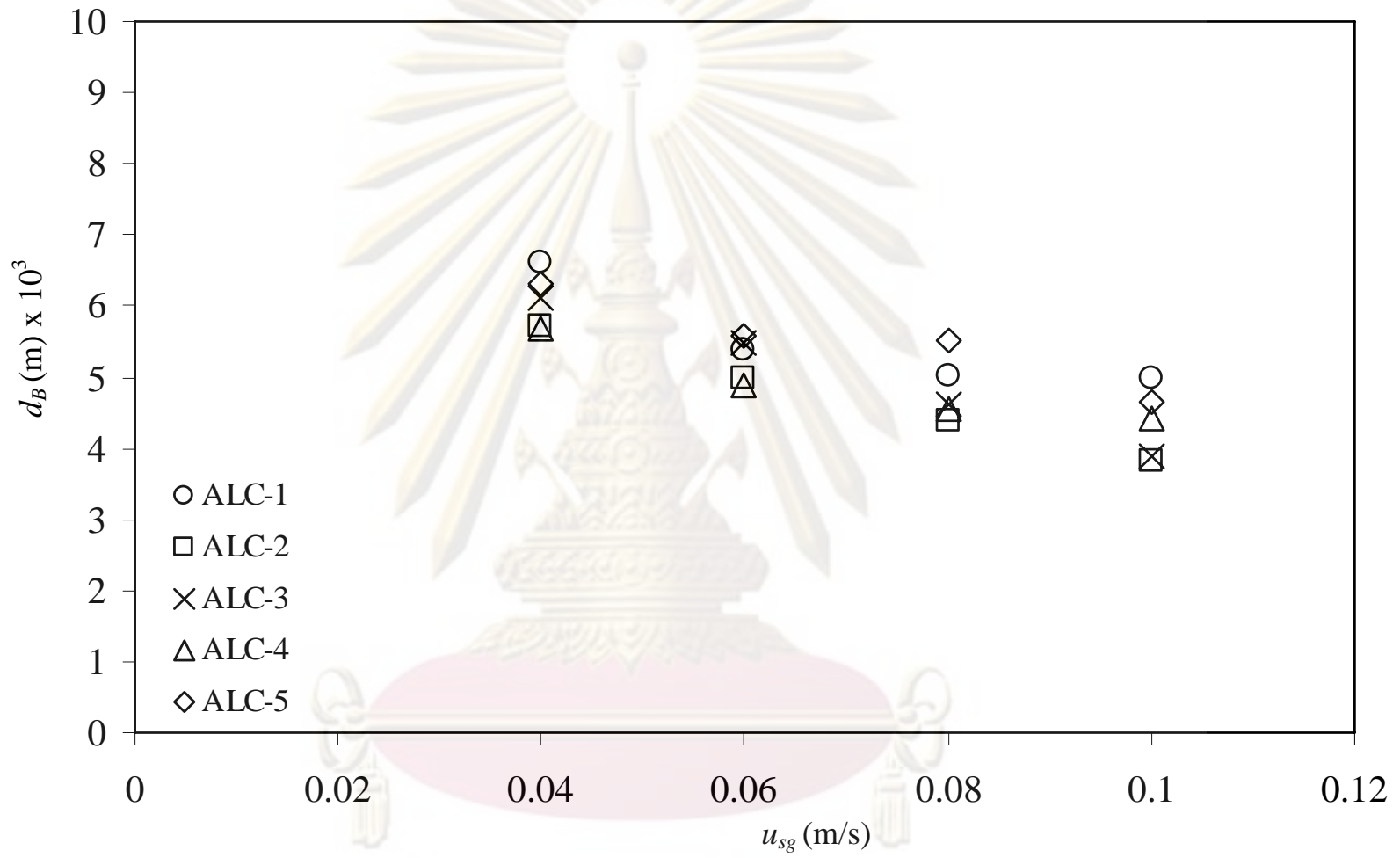


Figure 4.9 Relationship between average bubble diameter (d_{Bs}) and superficial gas velocity (u_{sg})

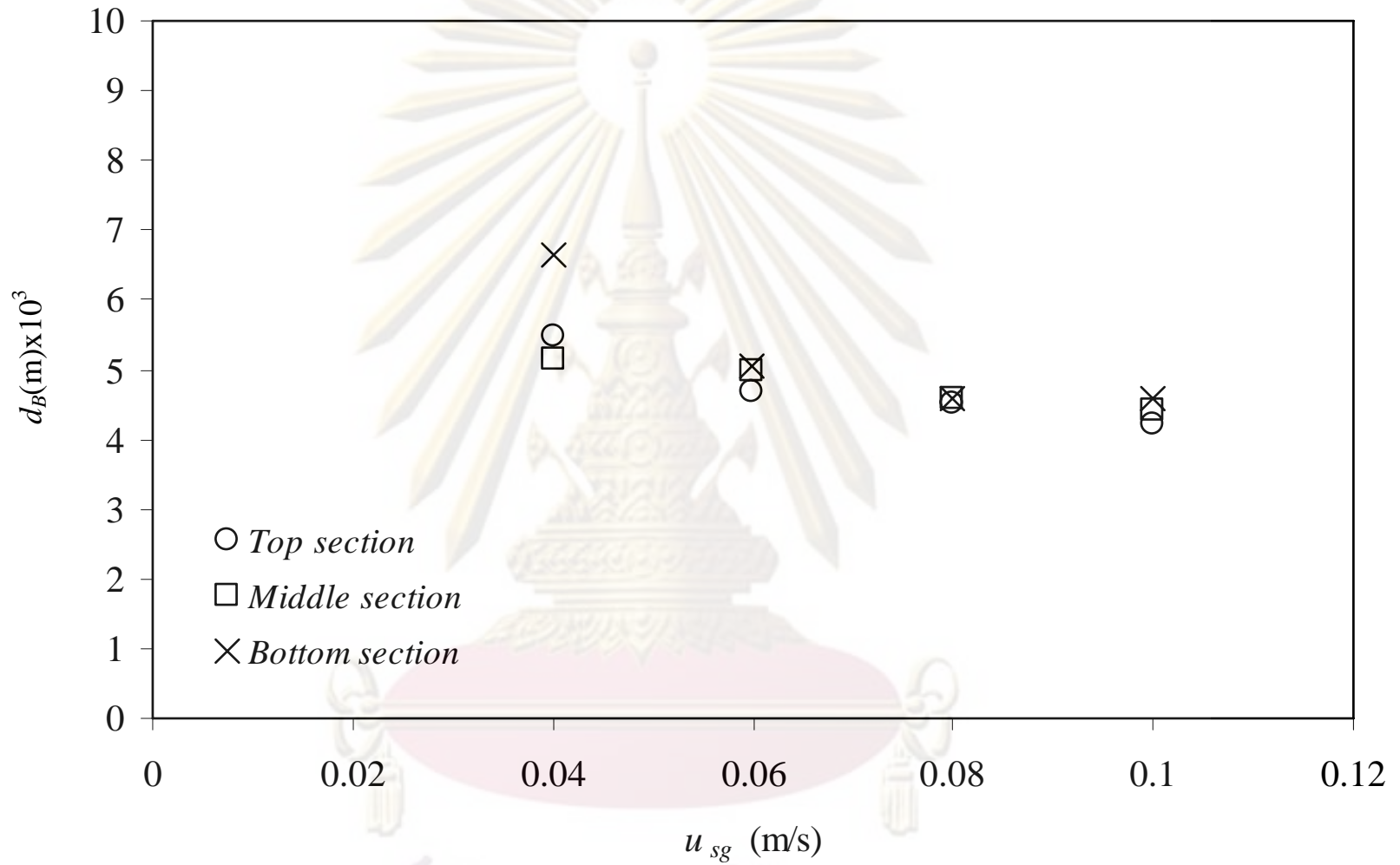


Figure 4.10 Relationship between different axial location and superficial gas velocity (u_{sg})

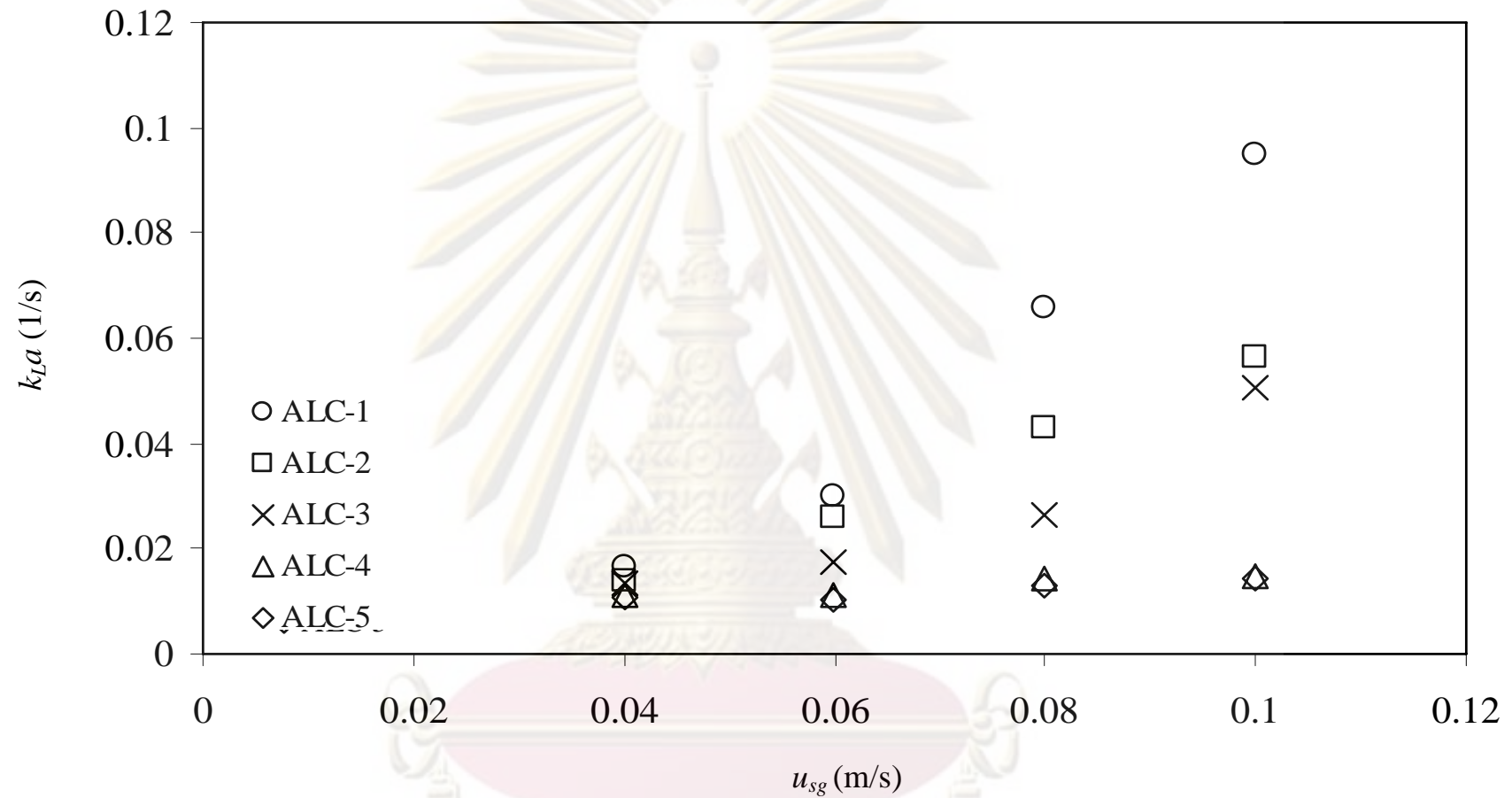


Figure 4.11 Relationship between the overall volumetric mass transfer coefficients (k_{La}) and superficial gas velocity (u_{sg})

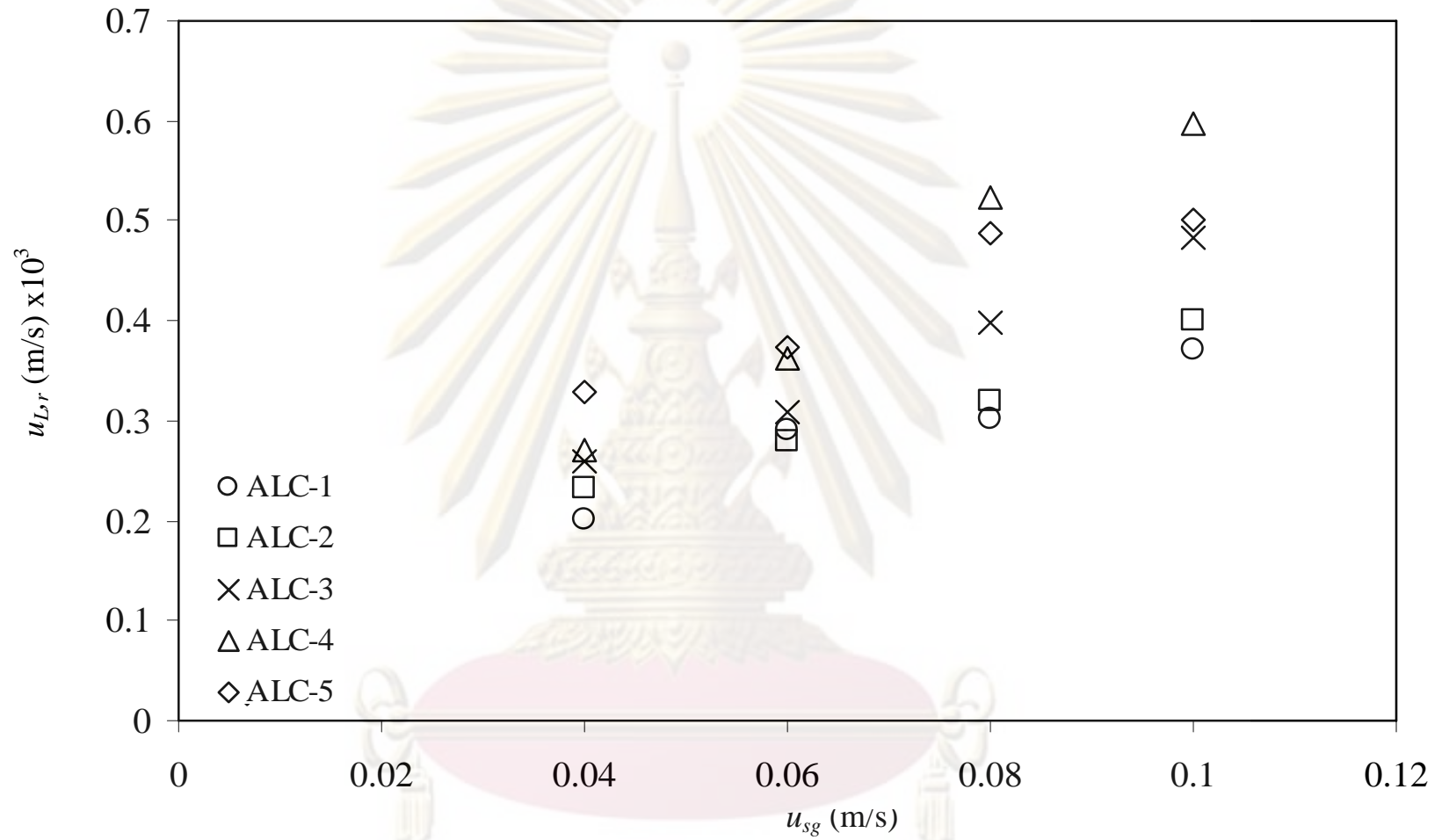


Figure 4.12 Relationship between the liquid velocity in riser ($u_{L,r}$) and superficial gas velocity (u_{sg})

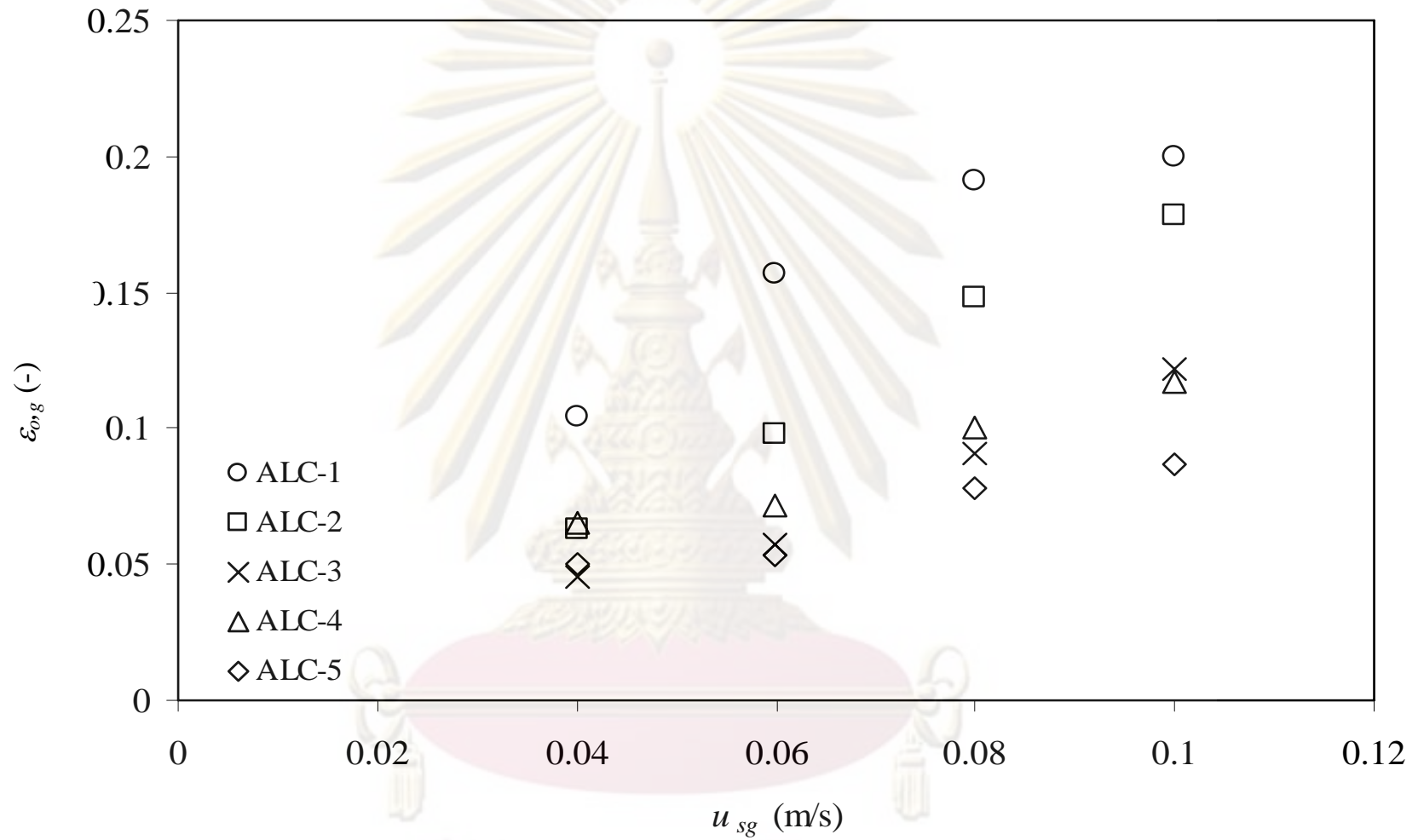


Figure 4.13 Relationship between the overall gas holdup ($\epsilon_{o,g}$) and superficial gas velocity (u_{sg})

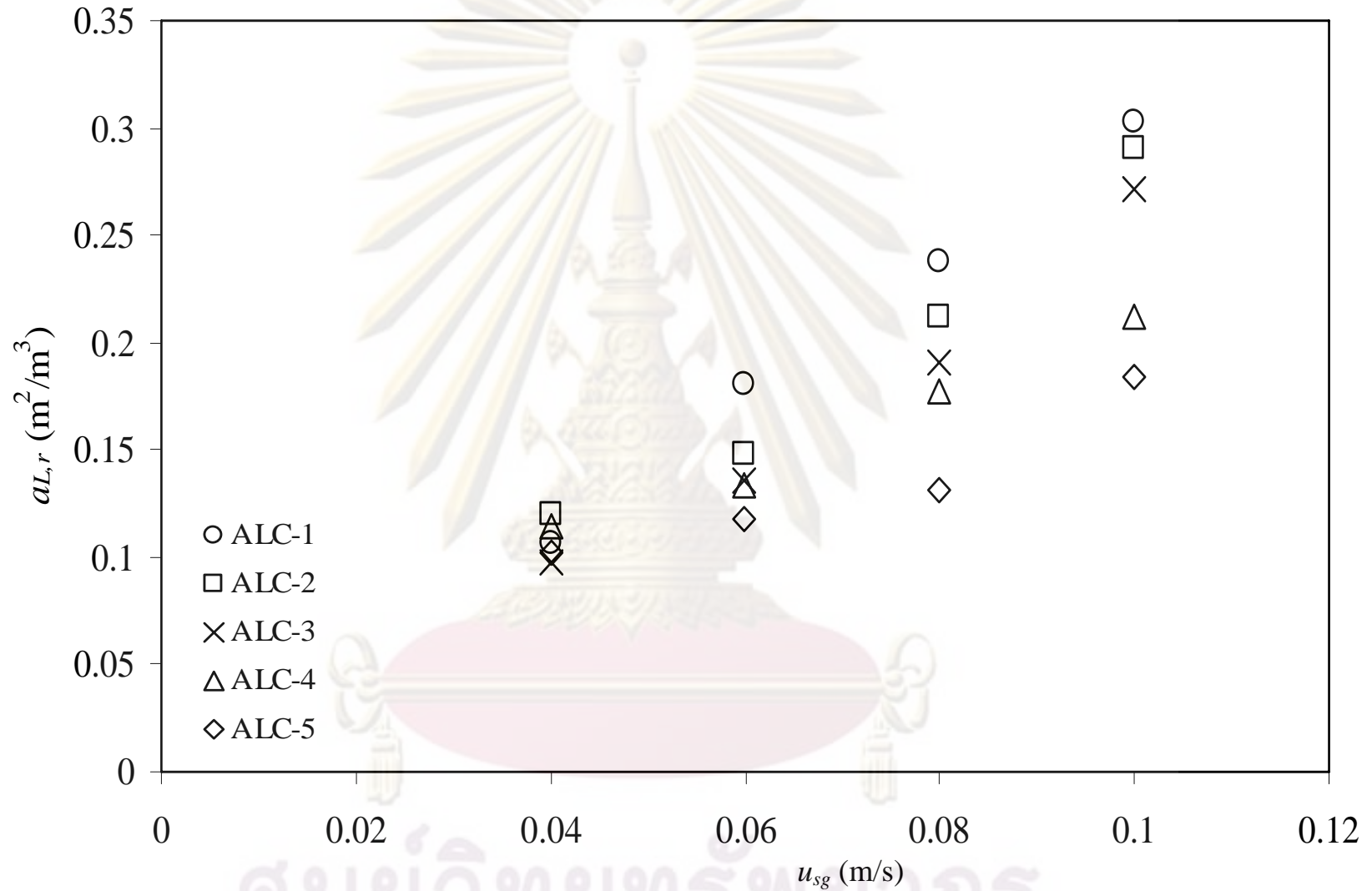


Figure 4.14 Relationship between specific interfacial area in riser ($a_{L,r}$) and superficial gas velocity (u_{sg})

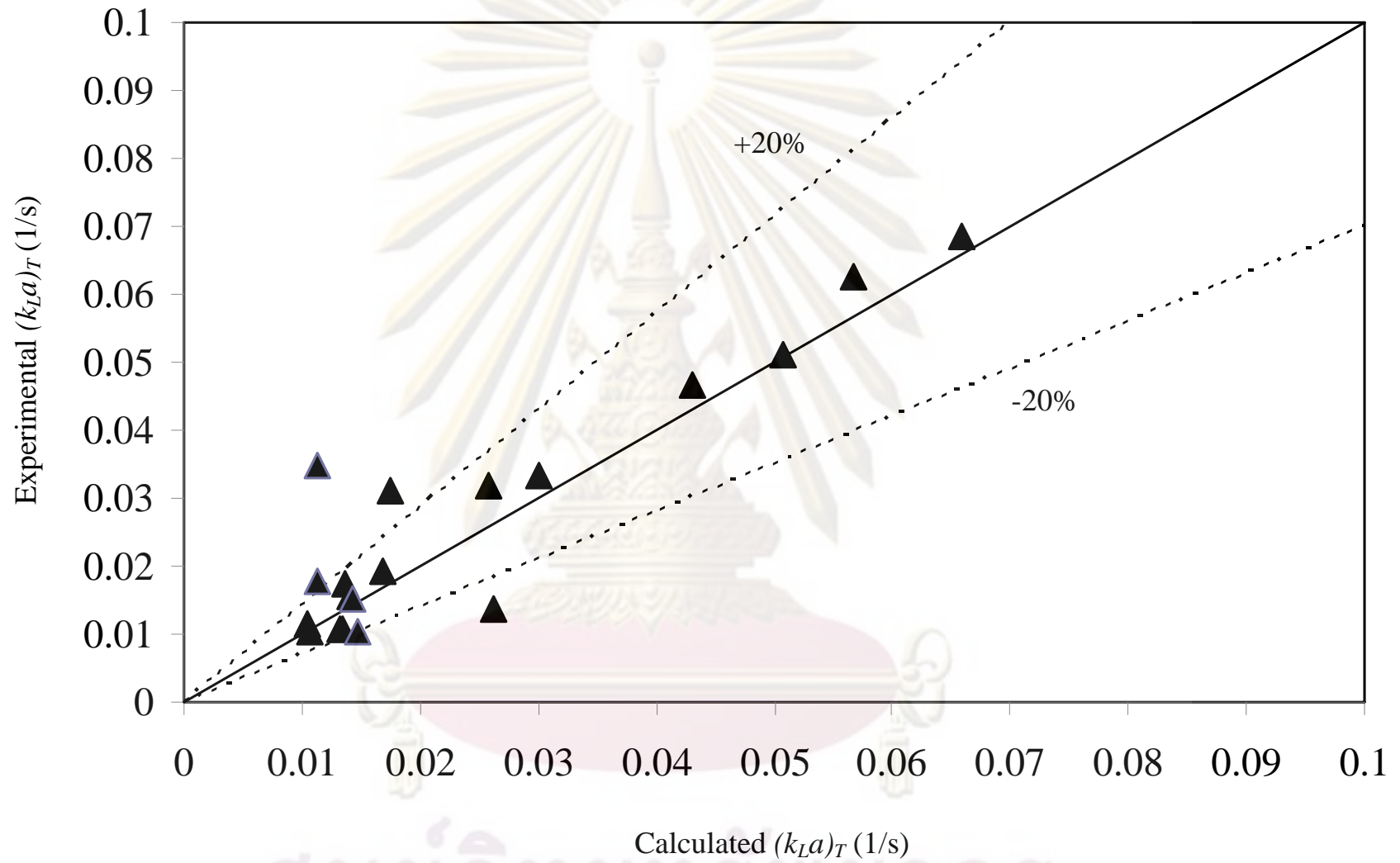


Figure 4.15 Comparison of overall volumetric mass transfer between experimental and calculation

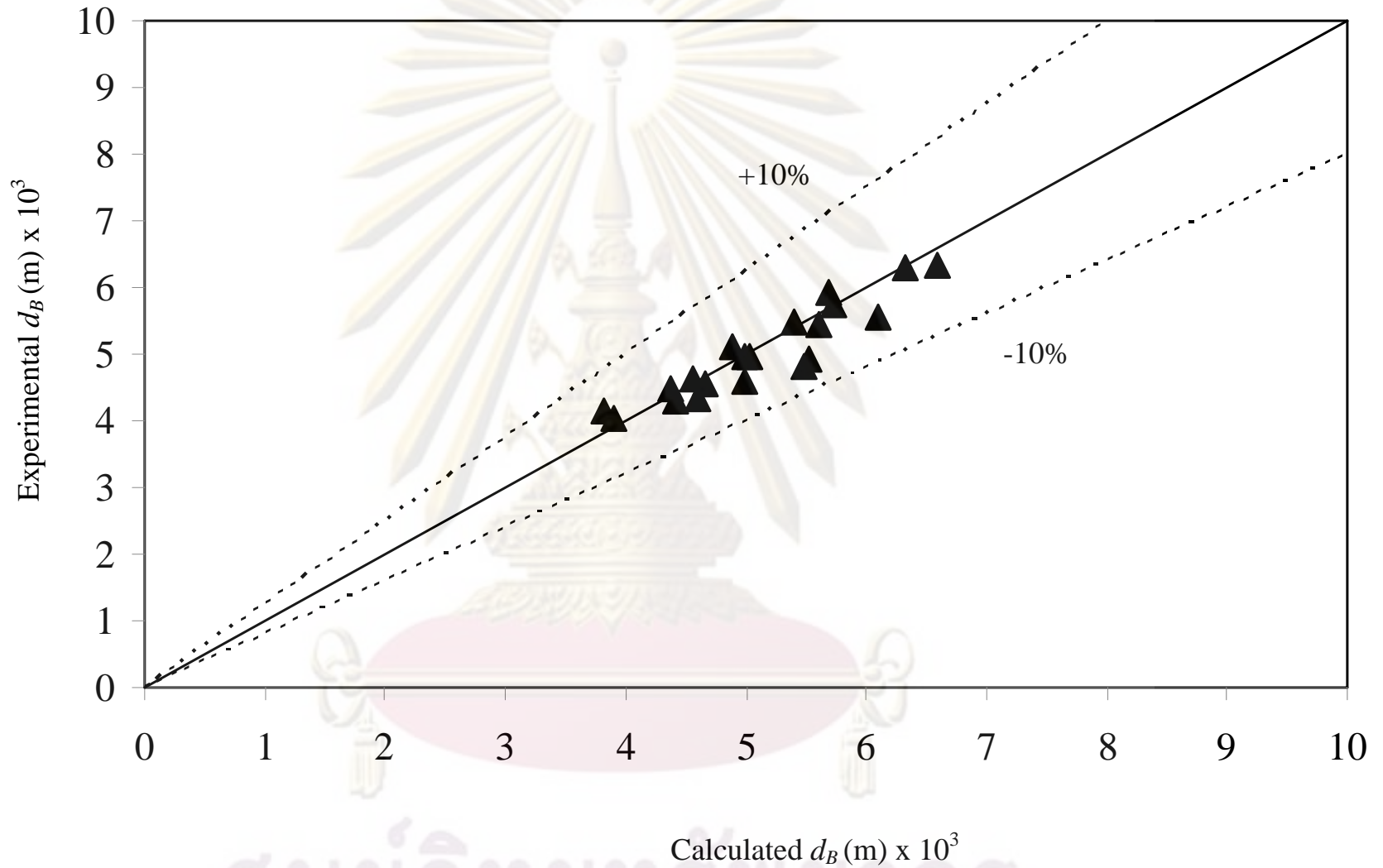


Figure 4.16 Comparison of experimental and calculation of Sauter mean diameter from Equation 4.16

CHAPTER 5

Conclusions, Contributions and Recommendations

5.1 Conclusions

The bubble size distribution is known to be one of the most important parameters in the airlift system regarding the gas-liquid mass transfer because it has significant influence on the specific interfacial area and the mass transfer coefficient. In practice, bubble size was measured in terms of the Sauter mean diameter (d_{Bs}) and this parameter was also affected by the configuration of the geometry of the reactor, including position of air sparger and ratio between cross-sectional areas of downcomer and riser. The sparger position has an influence on the contactor performance as it changed the flow pattern of the bubbles which affected the breakup and coalescence of the bubbles in the system.

Based on the various parameters that has influence on bubble size distribution as discussed earlier; the main conclusions can be presented as follows:

1. The bubble size distribution in the riser of all ALCs was a normal type with a narrow gap. The curve was found to have one main bubble size and their distribution seem to slightly change in the system.
2. The Sauter mean diameter of bubble in the system with sparger located at base of reactor was the smallest and this became larger when the sparger was located higher from the bottom of the reactor.
3. The Sauter mean diameter of bubble in the system decreased with an increasing superficial gas flow rate through the system.
4. The Sauter mean diameter of bubble in the system decreased with a decrease in the ratio between downcomer and riser cross-sectional area in the system.
5. The Sauter mean diameter of bubble in the system decreased along the column height.
6. In this study, the overall volumetric mass transfer coefficient increased with increasing superficial gas flow rate in the system.
7. The decrease in Sauter mean diameter enhanced the specific interfacial area, and thus, the overall volumetric mass transfer coefficient.

5.2 Contributions

Although airlift systems have been investigated quite intensively for the last decade, very little was known about the effect of sparger position on the system performance. This study is among the very few that disclosed such information. The results are therefore useful for the future design and adjustment of airlift contactors. To generalize the effect of the various parameters investigated in this work, a simplified mathematical model was proposed to predict the Sauter mean diameter of bubble within scopes of this work. The model was verified with a large set of experimental design which, to certain extent, was reliable and accurate.

5.3 Recommendations

In this work, the sparger was installed at base of column and introduce gas phase into the annular section. The flow pattern forced the air bubbles to move out of the center towards the wall of the reactor where breakage was observed. On the contrary, if the gas phase was sparged inside draft tube column, the results of hydrodynamics performance and bubble size distribution could be different. This is because the flow pattern, in this case, will push the bubbles towards the center of the reactor, and it is anticipated that bubble-bubble coalesce will occur instead of bubble-bubble breakup. This experiment is difficult to design as the measurement of bubble inside the draft tube with the photographic technique is not accurate and other measurement techniques must be developed, such as X-ray fluoroscopy, high-speed digital video camera, refractive optical probe and ultrasonic technique for improved the contrast image of bubble.

Having mentioned this, photographic method itself seems to have limitation in the annulus sparged airlift systems as visual observation becomes unclear even at low gas throughput. Future research should be directed towards the development of a simpler measurement technique for bubble size which would allow a more accurate estimate of most gas-liquid mass transfer parameters.

References

- Bailey J. E., and Ollis D. F., 1986. Biochemical Engineering Fundamentals Chemical Engineering Series .New York : McGraw-Hill.
- Blažej, J. Annuš and J.Markoš. 2004. Comparison of gassing-out and pressure-step dynamic methods for k_{La} measurement in an airlift reactor with internal loop. Chemical Engineering Research and Design 82: 1375-1382.
- Bozzano G. and Dente. 2001. Shape and terminal velocity of single bubble motion: a novel approach. Computer and Chemical Engineering 25: 571-576.
- Colella D., Vinci D., Bagatin R., Masi M. and Bakr A.E. 1999. A study on coalescence and breakage mechanisms in three different bubble columns. Chemical Engineering Science 54: 4767-4777.
- Chisti M. Y. 1989. Airlift bioreactors. NY: Elsevier Science Publishing.
- Chisti Y., Wenge F. and M.Y. Murray. 1994. Relationship between riser and downcomer gas hold-up in internal-loop airlift reactors without gas-liquid separator. Chemical Engineering Journal 57: B7-B13.
- Garcia-Ochoa, F. and Gomez, E. 2004. Theoretical of gas-liquid mass transfer coefficient, specific area and hold-up in sparged stirred tanks. Chemical Engineering Science 59: 2489-2501.
- Jamialahmadi, M., Branch, C., and Müller-Steinhagen. 1994. Terminal bubble rise velocity in liquids. Trans. Inst. Chem. Eng. PartA 72: 119-122.
- Kafarov V. 1985. Fundamental of Mass Transfer Gas-Liquid, Vapour-Liquid and Liquid-Liquid System, Second Edition. Moscow : Mir Publisher.

- Korpajarvi J., Oninas P. and Reunanen J. 1999. Hydrodynamics and mass transfer in an airlift reactor. Chemical Engineering Science 54: 2255-2262.
- K.-H. Choi, Y. Chisti and M. Moo-Young. 1996. Comparative evaluation of hydrodynamics and gas-liquid mass transfer characteristics in bubble column and airlift slurry reactor. Chemical Engineering Journal 62: 223–229.
- Lin T-J. and Po-Chou C. 2005. Studies on Hydrodynamics of an Internal-loop Airlift Reactor in Gas Entrainment Regime by Particle Image Analyzer. Chemical Engineering Journal 108: 69–79.
- Lu X., Ding J., Wang Y. and Shi J. 2000. Comparison of the hydrodynamics and mass transfer characteristics of a modified square airlift reactor with common airlift reactors. Chemical Engineering Science 55: 2257-2263.
- Luo H.-P. and Al-Dahhan M.H. 2008. Local characteristic in draft tube airlift bioreactor. Chemical Engineering Science 63: 3057-3068.
- Majumder S.-K., Gautam K. And Dibyendu M. 2006 Bubble size distribution and gas-liquid interfacial area in a modified down flow bubble column. Chemical Engineering Science 122: 1-10.
- Mario A. and Talaia. 2008. Terminal velocity of a bubble rise in a liquid column. International Journal Of Applied Science 4: 152-156
- Marrucci, G. 1965. Rising velocity of a swarm of spherical bubbles. Ind. Eng. Chem. Fundam 4: 224-225.
- Majumder S.-K., Gautam K. And Dibyendu M. 2006 Bubble size distribution and gas-liquid interfacial area in a modified down flow bubble column. Chemical Engineering Science 122: 1-10.

- Mehrnia M.R., Towfighi J., Bonakdarpour B., and Akbarnejad M.M. 2005. Gas hold-up and oxygen transfer in a draft tube airlift bioreactor with petroleum-based liquids. Biochemical Engineering Journal 22: 105-110.
- Merchuk J.C. 1986. Gas holdup and liquid velocity in a two-dimensional airlift reactor. Chemical Engineering Science 41: 11-16.
- Mir6n .S., Garca M.-C., Camacho F., Grma E. And Chisti Y. 2004. Mixing in bubble column and airlift reactors. Chemical Engineering Research and Design 82(A10): 1367-1374.
- Painmanakul P., Loube're K., Hebrard G., Mietton-Peuchot M., and Roustan M. 2005. Effect of Surfactants on Liquid-Side Mass Transfer Coefficients. Chemical Engineering Science 60: 6480 – 6491.
- Ruen-nagm D., Wongsuchoto P., Limpanuphap A., Charinpanitkul T. and Pavasant P. 2008. Influence of salinity on bubble size distribution and gas-liquid mass transfer in airlift contactors. Chemical Engineering Journal 141: 222-232.
- Shing L. and S-J. Hwang. 2003. Local hydrodynamics of gas phase in an internal-loop airlift reactor. Chemical Engineering Journal 91: 3-22.
- Skelland A.H.P. 1974. Diffusional Mass Transfer. New York: Wiley.
- Stanley M. 1998. An introduction to mass and heat transfer. New York: Wiley.
- Treybal R.E. 1980. Mass Transfer Operations. New York : McGraw-Hill.
- Wallis G.B. 1969. One Dimensional Two-Phase Flow. New York : McGraw-Hill.
- Welty, J.R., Wicks C.E., and Wilson, R.E. 1984. Fundamentals of Momentum, Heat, and Mass Transfer. New York: Wiley.

Wongsuchoto P., Charinpanitkul T., and Pavasant P. 2003. Bubble size distribution and gas-liquid mass transfer in airlift contactors. Chemical Engineering Journal 92: 81-90.

Wongsuchoto, P. and Pavasant, P. 2003. Internal liquid circulation in annulus sparged internal loop airlift contactors Chemical Engineering Journal 100: 1-9



ศูนย์วิทยทรัพยากร
จุฬาลงกรณ์มหาวิทยาลัย



APPENDICES

ศูนย์วิทยทรัพยากร
จุฬาลงกรณ์มหาวิทยาลัย



Appendix A

ศูนย์วิทยทรัพยากร
จุฬาลงกรณ์มหาวิทยาลัย

List of abbreviations and notations

Abbreviations

ALC	Airlift contactor
Gr	Grashof Number $\left(\frac{d_{Bs}^3 \rho_L \Delta \rho g}{\mu_L^2} \right)$
Re	Reynolds Number $\left(\frac{d_{Bs} v_s \rho_L}{\mu_L} \right)$
Sc	Schmidt number $\left(\frac{\mu_L}{\rho_L D_L} \right)$
Sh	Sherwood Number $\left(\frac{k_L d_{Bs}}{D_L} \right)$

Notations

a	Specific interfacial area [m ² /m ³]
A_d	Cross-sectional area [m ²]
c_o	Initial dissolved oxygen concentration [mg/l]
d_b	Bubble diameter [mm]
d_B	Sauter mean diameter [mm]
d_i	Sphere diameter with the same volume as ellipsoidal bubble [mm]
d_o	Orifice diameter [cm]
D	Gas diffusivity [m ² /s]
D_{ALC}	Airlift diameter [cm]
D_{dt}	Draft tube diameter [cm]
D_i	Inside draft tube diameter [cm]
D_{io}	Outer draft tube diameter [cm]
h	Video level [cm]
H	Height [cm]
g	Gravitational acceleration [cm/s ²]
k_L	Overall mass transfer coefficient [m/s]
k_{La}	Overall volumetric mss transfer coefficient [1/s]
N	Gas-liquid mass flux [mg/s.m ²]
N_i	Bubble number with an equivalent sphere diameter [-]
p	Major axes of bubble [mm]

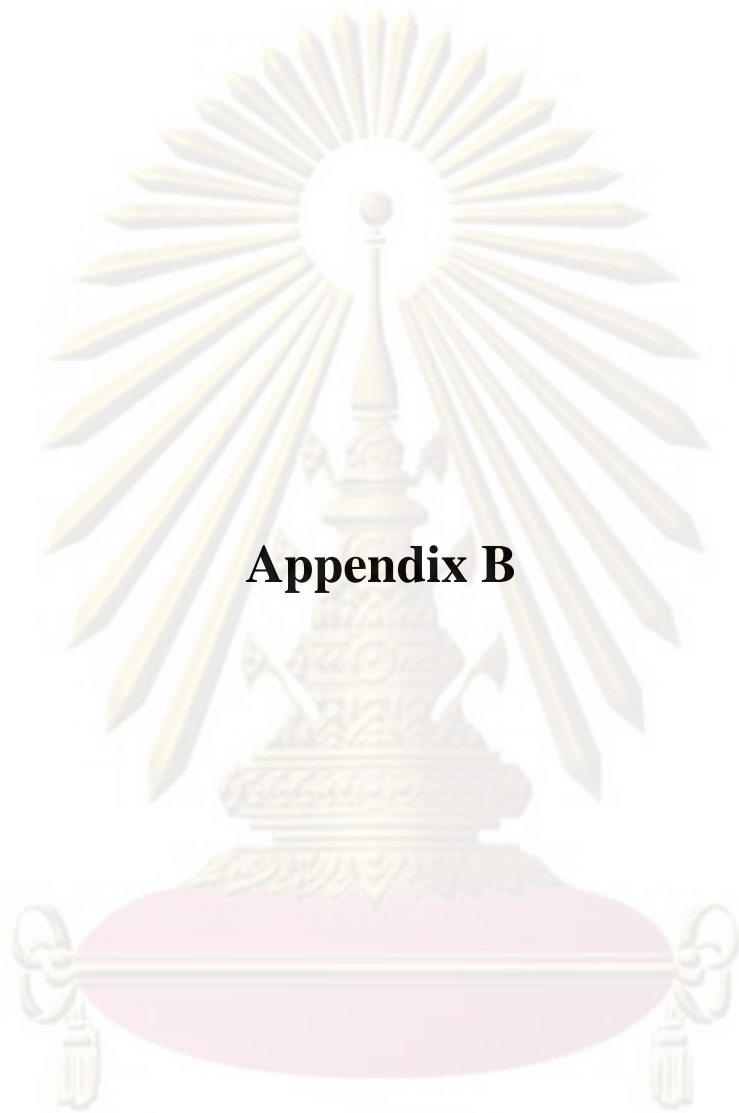
p_A	Partial pressure of molecule A [atm]
q	Minor axes of bubble [mm]
Q	Volumetric flow rate [m ³ /s]
t	Time [s]
u_{sg}	Superficial gas velocity [m/s]
U_B	Bubble rise velocity [m/s]
v	Liquid velocity [cm/s]
V	Volume [cm ³]
Z	Height of liquid level in manometer [cm]

Greek symbols

ε	Gas holdup [-]
δ	Film thickness [cm]
μ	Viscosity [Pa.s]
Π	Pi [-]

Subscripts

A	Molecule A
ALC	Airlift contactor
b	Bulk liquid
B	Molecule B
d	Downcomer
D	Dispersed liquid or aerated
dt	Draft tube
G	Gas phase
i	Interface
L	Liquid phase or unaerated
O	Overall
O_2	Oxygen
r	Riser
t	Gas-liquid separator



Appendix B

ศูนย์วิทยทรัพยากร
จุฬาลงกรณ์มหาวิทยาลัย

in conjunction with the

22nd SYMPOSIUM OF MALAYSIAN CHEMICAL ENGINEERS (SOMCHE)


15th REGIONAL SYMPOSIUM ON CHEMICAL ENGINEERING (RSCE)

INNOVATIONS FOR SUSTAINABLE FUTURE

Impiana KLCC Hotel & Spa,
Kuala Lumpur, Malaysia
2nd & 3rd December 2008

PROCEEDINGS
Volume I

Organized by:
Department of Chemical & Process Engineering,
Faculty of Engineering & Built Environment,
Universiti Kebangsaan Malaysia



in cooperation with: **Co-sponsored by:**

IChemE PETRONAS BASF PETRONAS CHEMICALS InnoBio

ศูนย์วิจัยทรัพยากร
จุฬาลงกรณ์มหาวิทยาลัย

EFFECT OF SPARGER POSITION ON BUBBLE SIZE DISTRIBUTION AND GAS-LIQUID MASS TRANSFER IN INTERNAL AIRLIFT CONTACTOR

Sond Bunsan and Prasert Pavasant*

Department of Chemical Engineering, Faculty of Engineering, Chulalongkorn
University,
Bangkok, 10330, Thailand

*Corresponding Author, Tel: +662 2218 6870, Fax: +662 2186877, email:
sondi2b@hotmail.com

Keywords: pneumatic reactor; reactor design; bubble column; hydrodynamic
behavior

ABSTRACT

The influence of sparger position and the ratio between cross-sectional areas of downcomer and riser (A_d/A_r) on bubble size distribution in the 17-L internal loop airlift contactor was described. The experiment was performed using superficial gas velocity, U_{sg} , of 3.92 and 9.62 cm/s. A photographic technique was used to measure the bubble size distribution. Experimental results revealed that the bubble size decreased with an increase in superficial gas velocity. Lowering sparger position (6 cm above the bottom) resulted in the formation of smaller bubble size. Accordingly, a higher overall gas holdup was observed at lower sparger position, and so was the overall volumetric mass transfer coefficient.

INTRODUCTION

Airlift contactors are widely employed in many biochemical processes such as aerobic fermentation and wastewater treatment. The main advantages of airlift reactors over bubble columns are improved mixing and actually higher mass transfer coefficients in some instances. In airlift reactors, the intrinsic complicated hydrodynamic structures induced by bubble motion have been recognized to be the key factor responsible for the mass transfers (Lin et al., 2005). Bubble size depends on contactor geometry, fluid properties, type of gas sparger and its position in an airlift contactor. Orifice diameters of the sparger have been shown to strongly influence the gas holdup in bubbles columns (Merchuk et al., 1986). Meanwhile, Wongsuchoto et al. (2003) showed that the average bubble size tended to increase with increasing orifice number of sparger. Moreover, Kilonzo et al. (2006) reported that the bottom clearance (spacing between the lower end of the baffle and the base plate of the reactor) had a strong

influence on the rate of liquid and gas circulation in an airlift contactor which could then significantly affect the overall gas holdup in an internal airlift contactor.

Up to now, there are only few studies on the effect of sparger position and its design on bubble size distribution in internal airlift contactors. The principle objective of this study is to investigate how hydrodynamic and mass transfer parameters, such as, bubble size distribution, gas holdup, and mass transfer coefficient in the airlift system were affected by the sparger position.

EXPERIMENTAL

Apparatus

A schematic diagram of experimental system is illustrated in Figure 1. The airlift contactor (ALC) consists mainly of an outer cylinder and a draft tube. The outer cylinder has a diameter of 13.7 cm, and the inner cylinder or the draft tube has a diameter of 10.11 cm, which makes the ratio between downcomer and riser cross sectional area of 1.40. All parts are made from transparent acrylic plastic to allow visual observation.

The draft tube is placed such that the bottom of the draft tube is 10 cm above the bottom of the column. The annular sparger made from PVC is installed at the base of the column to introduce the gas phase into the ALC. The influence of sparger position is examined by changing its position at 2 points, i.e. at 6 and 12 cm above the bottom of the column. Air flow rate is controlled by a calibrated rotameter and, is set in terms of superficial gas velocity or U_{sg} at 3.92 and 9.62 cm/s.

Bubble size distribution measurement

The measurements of the bubble size distribution are performed only in the riser of the internal loop ALC using a photographic technique method. The bubble sizes are measured at the middle part of the column about 50 cm above the bottom of the draft tube. The number of bubbles used in the measurement is more than 200 bubbles in each experiment. For ellipsoidal bubbles, the major and minor axes of bubble images are measured. The equivalent size of the bubble (d_B), representing the diameter of a sphere whose volume is equal to that of the bubble, is calculated using Eq. (1).

$$d_B = (p^2q)^{1/3} \quad (1)$$

Determination of hydrodynamic and mass transfer behavior of airlift contactors

The overall gas holdup, ε_o , is determined by the volume expansion method where:

จุฬาลงกรณ์มหาวิทยาลัย

$$\varepsilon_o = \frac{(H_D - H_L)}{H_D} \quad (2)$$

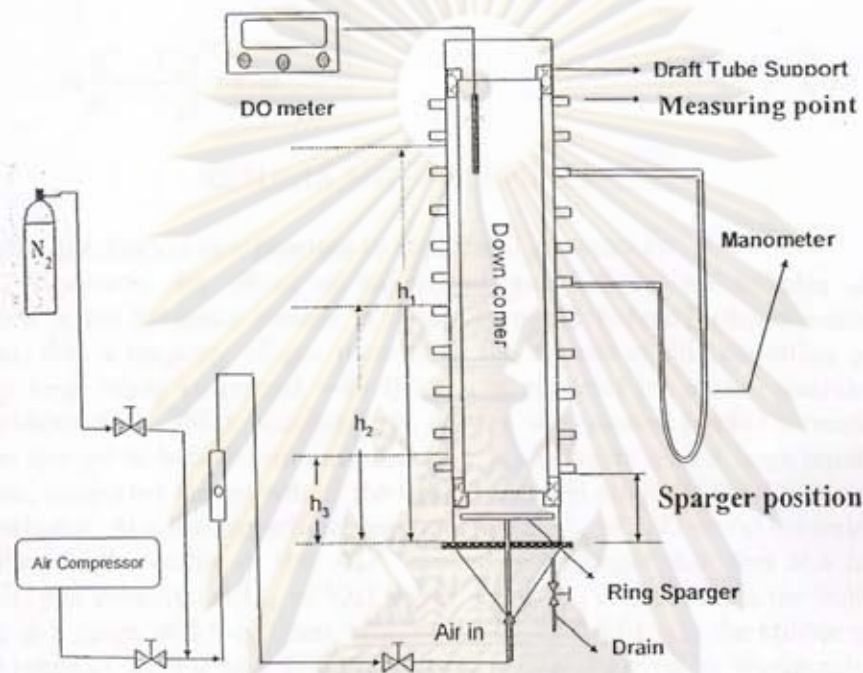


FIGURE 1 Schematic diagram of concentric internal loop airlift contactor employed in this work

The riser gas holdup, ε_r , is estimated by measuring the pressure difference, ΔP , between the two pressure taps located along the height of the column, Δh where:

$$\varepsilon_r = 1 - \frac{\Delta P}{\rho_L g \Delta H} \quad (3)$$

It is assumed that gas holdup in the top section is approximately equal to that in the riser, and therefore, the downcomer gas holdup, ε_d , can be computed from:

$$\varepsilon_{Gd} = \frac{\varepsilon_{Gr} H_D (A_d + A_r) - (H_D A_d + H_D A_r - H_d A_d) \varepsilon_{Gr}}{H_d A_d} \quad (4)$$

จุฬาลงกรณ์มหาวิทยาลัย

The overall volumetric mass transfer coefficient ($k_L a$) is determined by the dynamic method. A dissolved oxygen meter is used to record the changes in oxygen concentration with time in the ALC. The system is initially freed of O_2 by bubbling N_2 through the liquid for approx. 10 min. The calculation of $k_L a$ follows Eq. (5):

$$\ln \frac{(C^* - C_o)}{(C^* - C_t)} = k_L a t \quad (5)$$

RESULTS AND DISCUSSION

Bubble size distribution as a function of superficial gas velocity

Figure 2 illustrates the effect of superficial gas velocity on bubbles size distribution in the air-water system. It should be noted, before further discussed this point, that a majority of gas bubbles in the system at this condition was relatively large when compared with the results reported by other researchers (Wongsuchoto et al. 2003). Kazakis et al. (2007), who studied bubble formation in porous sparger in bubble columns, reported that spargers with a large number of orifices, supported the growth of the bubble and this might be the situation in this experiment. At a low superficial gas velocity (at U_{sg} of 3.92 cm/s) the bubble size at the middle section of this ALC seemed to be larger than that at a high superficial gas velocity (at U_{sg} of 9.62 cm/s), i.e. at U_{sg} of 3.92 cm/s, the bubble size was in a range of 5.0-6.0 mm, whereas at U_{sg} of 9.62 cm/s, the bubble size was in a range of 4.0-5.0 mm. This was similar to that observed by Wongsuchoto et al. (2003) who reported that bubble size decreased with increasing superficial gas velocity in the airlift systems.

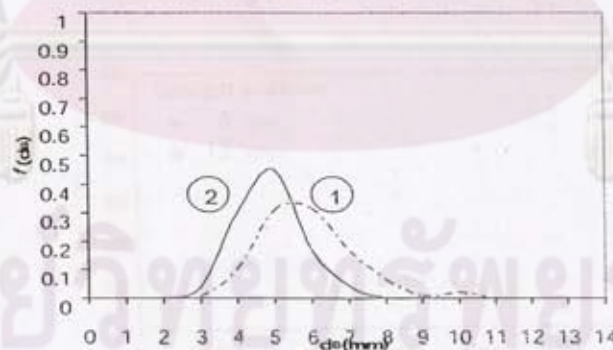


FIGURE 2 Frequency distribution of bubble sizes at various U_{sg} : (1) $U_{sg} = 3.92$ cm/s and (2) U_{sg} equal to 9.62 cm/s

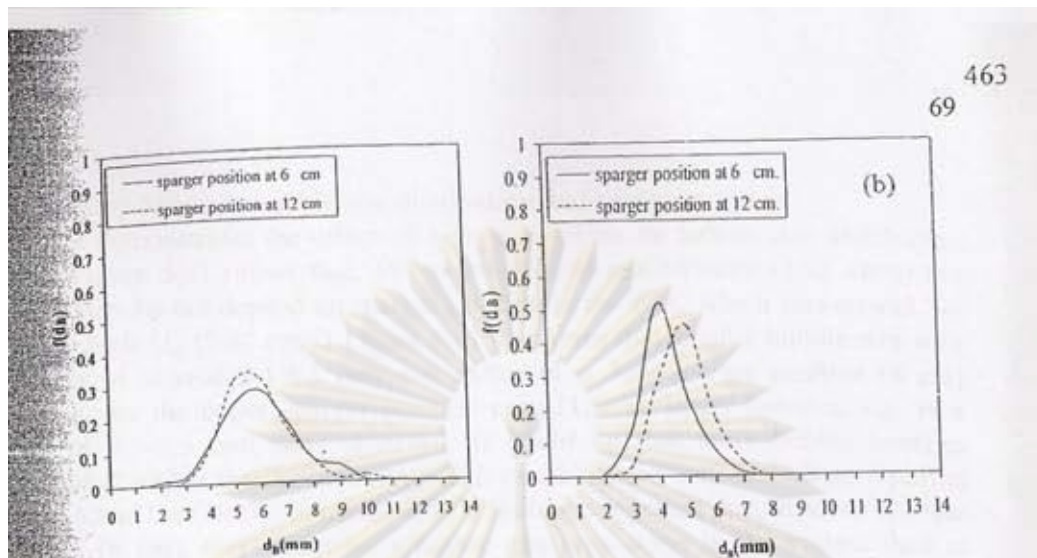


FIGURE 3 Effect of sparger position on bubble size distribution at various U_{sg} : (a) $U_{sg} = 3.92$ cm/s and (b) U_{sg} equal to 9.62 cm/s

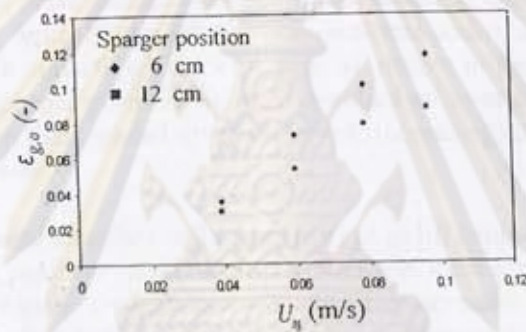


FIGURE 4 Relationships between the overall gas holdup, $\epsilon_{g,o}$ and superficial gas velocity, U_{sg} (cm/s) at various sparger positions

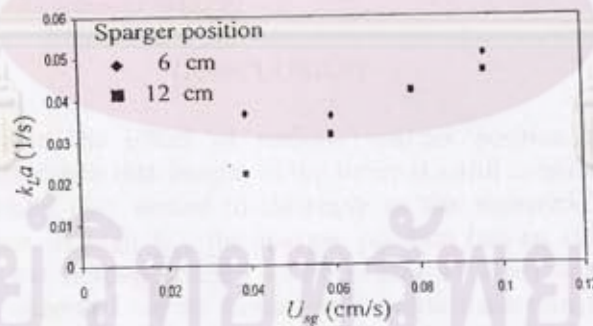


FIGURE 5 Relationships between the overall volumetric mass transfer coefficient, $k_L a$ and superficial liquid velocity, U_{sg} (cm/s) at various sparger positions

Relationship between bubble size distribution and sparger position

Figure 3 demonstrates the effect of sparger position on bubble size distribution where Figure 3(a) shows that, at low superficial gas velocity (3.92 cm/s) the bubble size did not depend on sparger position in the ALC which was around 5-6 mm. At high U_{sg} (9.62 cm/s), Figure 3(b) illustrates that smaller bubble size with diameter of around 3.5-4.5 mm was obtained at low sparger position (6 cm) whereas, for the upper sparger position case (12cm), larger bubbles, e.g. in a range of 4.5-5.5 mm, was observed. It could be that more bubble breakup occurred at higher than at lower u_{SG} . This result agreed well with those reported by Zhao and Ge (2007). In addition, this finding suggested that, at lower sparger position (6 cm), there must be a higher gas proportion in the system than at higher sparger position (12 cm).

Overall gas holdup ($\epsilon_{g,o}$) in airlift contactor

Figure 4 describes the relationships between the overall gas holdup, $\epsilon_{g,o}$, and gas sparger position. As typically found for conventional airlift systems, the gas holdup increased with superficial velocity, and as shown in the this figure, $\epsilon_{g,o}$ was higher at lower sparger position. Sparger installed at lower position provided smaller bubbles which then moved at lower speed, increasing the residence time and holdup in the system.

Overall volumetric mass transfer coefficient (k_La) in airlift contactor

The effect of sparger position on the overall volumetric mass transfer coefficient, k_La , is illustrated in Figure 5 which revealed that k_La increased with an increase in U_{sg} . Similar to the gas holdup, lowering sparger position could enhance the overall volumetric mass transfer coefficient. As stated earlier, at lower sparger position, there existed more gas bubble recirculation in the system, hence, more surface area for gas-liquid mass transfer was obtained and this resulted in a higher gas-liquid mass transfer rate.

CONCLUSION

This work illustrated the effect of various sparger position and operating parameters on bubbles size distribution in the internal airlift contactor. This study indicated that bubbles size tended to decrease as the superficial gas velocity increased. Moreover, at high U_{sg} , the sparger position had an effect on bubble size. The overall gas holdup seemed to be higher at lower sparger position. Similar trend was observed for the overall volumetric mass transfer coefficient. The finding from this work could be used as a fundamental for the design of the internal airlift contactors.

Nomenclature

a	Specific interfacial area (m^2/m^3)
A_d	Cross-sectional area (m^2)
c_o	Initial dissolved oxygen concentration (mg/l)
d_b	Bubble diameter (mm)
d_B	Sauter mean diameter (mm)
d_i	Sphere diameter with the same volume as ellipsoidal bubble (mm)
h	Video level (cm)
Δh	Distance between pressure measurement points (m)
ΔP	Hydrostatic pressure different between two measuring point (N/m^2)
H	Height (cm)
$k_L a$	Overall volumetric mass transfer coefficient (1/s)
t	Time (s)
u_{sg}	Superficial gas velocity (cm/s)

Greek symbols

$\varepsilon_{g,o}$	Overall gas holdup (-)
ε_r	Riser gas holdup (-)
ε_{Gd}	Downcomer gas holdup (-)

REFERENCES

- Kazakis N.A., Mouza A.A. and Paras S.V., 2008. Experiment study of bubble formation at metal porous spargers: Effect of liquid properties and sparger characteristics on the initial bubble size distribution. *Chem. Eng. J.* **137**: 265-281.
- Kilonzo P.M., Margaritis A., Bergougnou M.A., Yu J.T. and Qin Y., 2006. Influence of the baffle clearance design on hydrodynamics of a two riser rectangular airlift reactor with inverse internal loop and expanded gas-liquid separator. *Chem. Eng. J.* **121**: 17-26.
- Lin T.-J., and Po-Chou C., 2005. Studies on Hydrodynamics of an Internal loop Airlift Reactor in Gas Entrainment Regime by Particle Image Analyzer. *Chem. Eng. J.* **108**: 69-79.
- Merchuk J.C., 1986. Gas holdup and liquid velocity in a two-dimensional airlift reactor. *Chem. Eng. J.* **41**: 11-16.
- Wongsuchoto P., Charinpanitkul T., Pavasant P., 2003. Bubble size distribution and gas-liquid mass transfer in airlift contactors, *Chem. Eng. J.* **92**: 81-90.
- Zhao H. and Ge W., 2007. A theoretical bubble breakup model for slurry beds or three-phase fluidized beds under high pressure, *Chem. Eng. J.* **62**: 109-115.

BIOGRAPHY

Miss. Sond Bunsan was born on 19th July, 1985 in Bangkok. Her native home was Ayutthaya province. She finished her secondary school from Jomsurang Upathum School in 2003. She got bachelor degree from Chemical Engineering in Faculty of Engineer at Thammasat University in 2006. She continued her further study for master's degree in Chemical Engineering at Chulalongkorn University. She participated in the Biochemical Engineering Research Group and achieved completed her Master's degree in October, 2009.



ศูนย์วิทยทรัพยากร
จุฬาลงกรณ์มหาวิทยาลัย